THE EFFECT OF TELECONNECTIONS ON NORTH ATLANTIC TROPICAL CYCLONE PRECIPITATION

A Thesis

by

YUE WANG

Submitted to the Office of Graduate and Professional Studies of
Texas A&M University
in partial fulfillment of the requirements for the degree of

MASTER OF SCIENCE

Chair of Committee,	Steven M. Quiring
Committee Members,	Oliver W. Frauenfeld
	Robert Korty
Head of Department,	David M. Cairns

May 2015

Major Subject: Geography

ABSTRACT

This study identified how tropical cyclone precipitation (TCP) in the North Atlantic (NAT) varies in space and time. It also determined how climatic oscillations influence TCP in the NAT using 14 years of satellite-derived (TRMM) precipitation data. The analysis focused on the entire NAT as well as the Gulf of Mexico (GMX), Caribbean (CAR), and East Coast (ECO) sub-basins. Tropical cyclones (TC) contributed a mean of 76 mm of precipitation per year in the NAT. TCP is generally higher in the western and central NAT and little TCP occurs in the eastern NAT and south of 15°N latitude. The highest mean annual TCP occurs in the Gulf of Honduras (333 mm). Although there is substantial interannual variability in TCP, no statistically significant trends was detected in TCP volume, total rainfall, and TCP fraction in the NAT between 1998 and 2011. TCP is strongly correlated with TC frequency and intensity. Seasons with more frequent and intense TCs also receive more TCP.

The relationship between TCP and four climate oscillations (El Niño/Southern Oscillation (ENSO), North Atlantic Oscillation (NAO), Quasi-Biennial Oscillation (QBO) and Atlantic Meridional Mode (AMM)) was evaluated. AMM has the strongest influence on TCP, especially in the CAR region. The positive phase of AMM is related to increased TCP. NAO also has an influence on TCP, but the sign of the relationship varies by sub-basin because NAO influences the movement of TCs. TCP tends to increase (decrease) in the CAR (ECO) when NAO is positive. Although ENSO has an influence on TCP in NAT, it is not as strong as AMM or NAO. TCP is enhanced during

La Niña phase and suppressed during El Niño phase. There is no obvious correlation between TCP and QBO.

ACKNOWLEDGEMENTS

I would like to thank many people who have assisted and supported me throughout my times in Texas A&M University.

First, I want to express appreciation and thanks to my advisor Dr. Steven Quiring. He is the one taught me the method of doing research, gave me priceless suggestions and cheered me up. His encouragement and patience are significant to me.

Also, I want to thank Dr. Oliver W. Frauenfeld and Dr. Robert Korty for serving as my committee members. They gave me some great comments and suggestions.

Special thanks to my parents. I would not be able to fly over the Pacific Ocean and have a wonderful experience here without their support. They are always standing by me. Thank you for your love and I love you. I am thankful to my friends in the Department of Geography and everybody at CSL. I enjoyed the time spending with you guys.

TABLE OF CONTENTS

Page

CHAPTER

LIST OF FIGURES

FIGURE Page

LIST OF TABLES

TABLE Page

CHAPTER I

INTRODUCTION

1.1 Motivation

Tropical cyclones (TC) threaten human life and can cause great economic losses worldwide (Landsea et al. 2008; Emanuel 2013). Swill (2010) found that seven of the ten most costly global natural disasters between 1970-2009, in terms of insured losses, were hurricanes that affected the Atlantic coast region of the United States, and the Gulf of Mexico. Even though the projected TC activity changes as a result of global climate change are still a matter of debate, research in terms of dynamical and thory models predicts that global warming will increase TC intensity, while the TC frequency will remain constant or decrease (Knutson et al. 2010). Past research has demonstrated that variations in North Atlantic TC intensity, frequency, cyclogenesis and movement can be related to regional and remote climate oscillations (Henderson et al. 1998; Knutson et al. 2010). TC and their remnants can produce significant precipitation as well as severe flooding. Flooding is one of the main causes of TC-related deaths within the United States (Rappaport 2000). However, relatively few studies have examined the patterns and variability TC precipitation in the North Atlantic. The role of the climate variability and its influence TC precipitation (TCP) also needs to be identified. This research will evaluate variations of TCP in the North Atlantic, develop a TCP climatology and investigate trends in TCP.

1.2 Research Objectives

The objectives of this thesis are:

1. Develop a TCP climatology in the North Atlantic to document the temporal and spatial patterns of TCP.
2. Determine how climatic oscillations influence TCP in the North Atlantic.

To achieve objective 1, 14 years the high resolution TRMM (Tropical Rainfall Measuring Mission) data will be used. In objective 2, statistical models will be developed to characterize how local and remote climate forcings influence TCP in the North Atlantic. Plausible physical mechanisms will be identified to explain why teleconnection patterns influence TCP.

CHAPTER II

LITERATURE REVIEW

2.1 Measuring TCP

The focus of this thesis is TC precipitation (i.e., precipitation directly attributable to tropical cyclones). It can result from the spiral rainbands associated with TCs and interactions between TCs and other weather systems. As shown in Figure 2.1, the distribution of rainfall varies in different regions of TC (Lonfat et al. 2004; Zhu and Quiring 2013). Past research has attempted to develop a standardized methodology for identifying and quantifying TCP based on distance from circulation center, the duration of the storm, and metrics of precipitation. For example, Englehart and Douglas (2001) show that in ninety percent of cases, precipitation occurs within a 550-600 km radius from the TC center. A distance of 500 km from the center of TC is commonly used (Lonfat et al. 2004; Dare et al.2012). Time is another variable that needs to be determined when measuring TCP. Sometimes, it is difficult to determine whether rainfall is associated with TC activity or whether it is due to other factors (e.g., enhanced monsoonal flows) (Cheung et al. 2008). Some past studies have adopted 6 hours before or after the full-orbit observation time and some identify a TC day (Yokoyama and Takayabu 2008; Rodgers et al. 2000). There are also different precipitation metrics that are used to measure TCP. Both rain rate (Kubota and Wang 2009) and accumulated rainfall amount are commonly used (Rodgers et al. 2000).

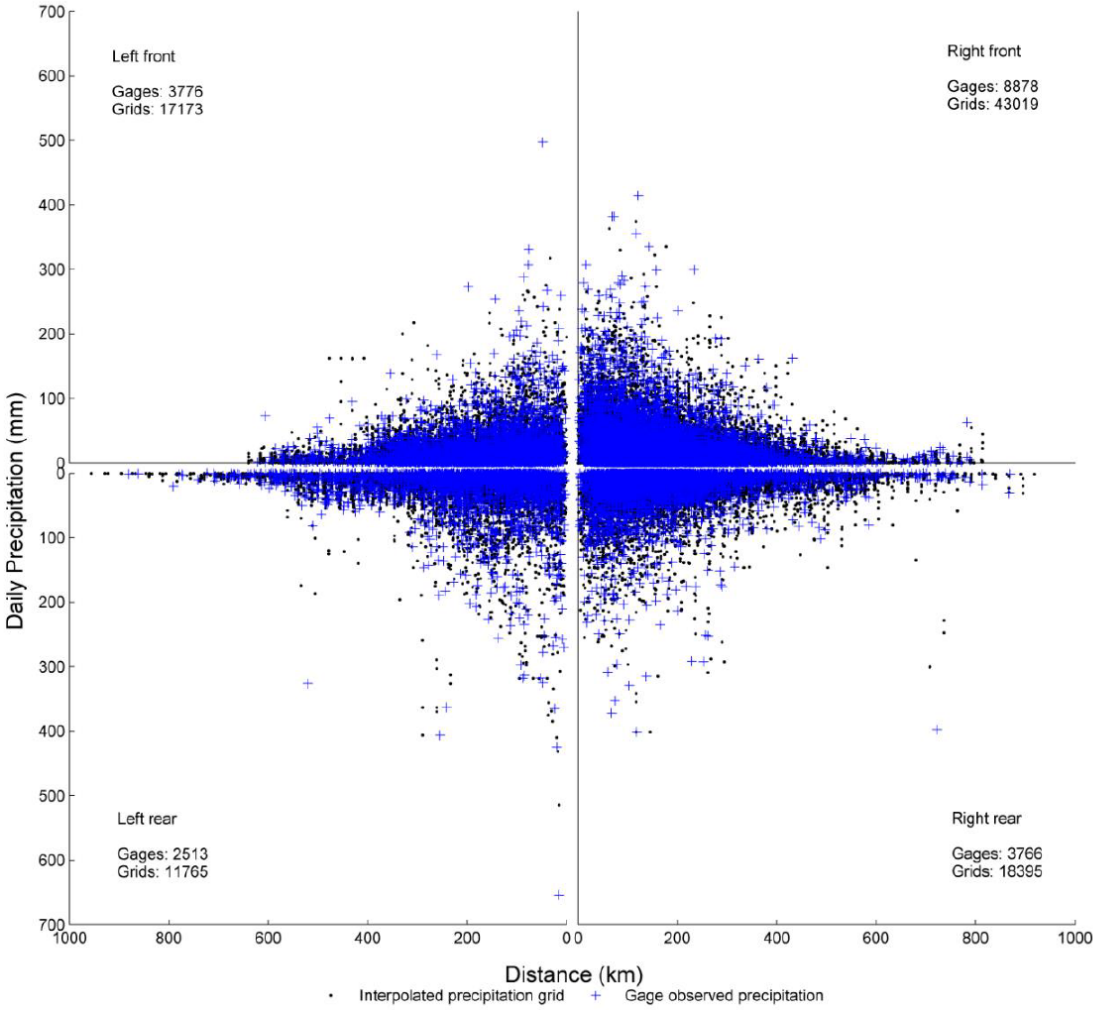

Figure 2.1. Distribution of daily precipitation (mm) (interpolated and gage-based) by quadrant with respect to the direction of movement and center of the TC (Source: Figure 4 in Zhu and Quiring, 2013).

2.2 Sources of TCP Data

There are four main sources of TCP data. Station-based rainfall observations provide a long-term and relatively accurate record of TCP (Kunkel et al. 2010; Chen et al. 2010). However, there are relatively few stations in and around the ocean basins where the majority of TCP occurs. The stations that are used to measure TCP typically come from islands or coastal locations. Also, because rain gauges only provide a point measurement it is necessary to have a high density rain gauge network that characterizing the spatial variability of TCP. This is not typically practical or economical (Grimes et al., 1999).

There are two sources of precipitation rainfall data that are commonly used in TCP studies: Tropical Rainfall Measuring Mission (TRMM) and Special Sensor Microwave Imager (SSM/I). TRMM provides rainfall measurement in tropical and subtropical regions. TRMM uses a unique combination of instruments to measure the three-dimensional structure of the rainfall field at a high resolution in both the horizontal and vertical. TRMM was designed only for rainfall observation and provides excellent coverage of the tropics from a low-inclination orbit (Adler et al. 2000, Simpson et al. 1988). TRMM uses Precipitation Radar (PR) to monitor rainfall by identifying storm structure. The TRMM Microwave Image (TMI) quantifies intensity of precipitation by measuring microwave energy. TRMM Visible and Infrared Scanner (VIRS) is a kind of indirect indictor of precipitation by sensing radiation in the visible to infrared. Clouds and the Earth's Radiant Energy Sensor (CERES) of TRMM is used to measure the energy of top of the atmosphere and energy budget over the tropical and subtropical

region. Also, TRMM's Lightning Imaging Sensor (LIS) is used to detect and locate lighting (Adler et al. 2000; Schumacher and Houze 2003, Kummerow et al. 2000). There are several TRMM rainfall algorithms used to convert radar reflectivity to rainfall rates. Among these products, 3B42 has the highest resolution in both time (3 hourly) and space (0.25 degree x 0.25 degree). Therefore, TRMM 3B42 is commonly used for evaluating TC precipitation. One limitation of TRMM is that data are only available since 1998 and observations are limited to tropical and sub-tropical regions. The SSM/I satellite has also been used to measure TCP. SSM/I scans conically at a 45° angle from nadir and it has an observational swath width of about 1400 km at the earth's surface (Rodgers et al. 2000). Based on a cloud-model, the relationship between brightness temperature and rain rate are calculated (Adler et al. 1991). The algorithm makes use of the high spatial resolution (15 km x 15 km) in SSM/I channels to measure rainfall amount. The character of SSM/I is quite similar to TRMM: high resolution but relatively less accurate than gauges, the observation region is limited due to fixed orbits. SSM was launched a few decades ago, however, the rainfall algorithm was changed in 1988. Therefore, most research utilizes the SSM/I data of rainfall observation after 1988 the post-SSM period (Rodgers et al. 2000; Lau et al. 2008).

A fourth source of TCP data is from merged products such as the Global Precipitation Climatology Project (GPCP). GPCP combines operational satellite microwave rainfall data, infrared data and surface rain gauge observations. These products are useful because they can improve the accuracy of satellite data and enhance the spatial coverage of station data (Lau et al. 2008; Ren et al. 2006). The primary GPCP

product is monthly precipitation data on a 2.5 ° global grid from the year of 1979 to the present (Adler et al. 2003). These data are useful for climate studies (Xie et al. 2003).

2.3 Spatial Variation of TC Precipitation

A number of previous studies have investigated spatial variations in TCP. Jiang and Zipser (2010) identified how TCs contribute to annual precipitation in six ocean basins: Northwest Pacific (NWP), East-central Pacific (EPA), South Pacific (SPA), Atlantic (ATL), North India Ocean (NIO) and South Indian Ocean (SIO). The NWP basin has the greatest TCP and largest TC rain fraction. Jiang and Zipser (2010) found that the TC frequency and intensity in the NWP are greater than the other five basins. TCP contributed 5% of the total rainfall in ATL, which is less than NWP, but greater than other basins. Jiang and Zipser (2010) found that increases in TCP were associated with higher TC frequency and larger TC size. In terms of global sub-basins, the largest TCP fraction occurs near the west of the Australia coast, southwest of the Baja California coast and the region around Taiwan Island and northeast of the Philippine Islands. In the north Atlantic, the largest TCP fractions are found in the western Gulf of Mexico and central North Atlantic (Figure 2.2).

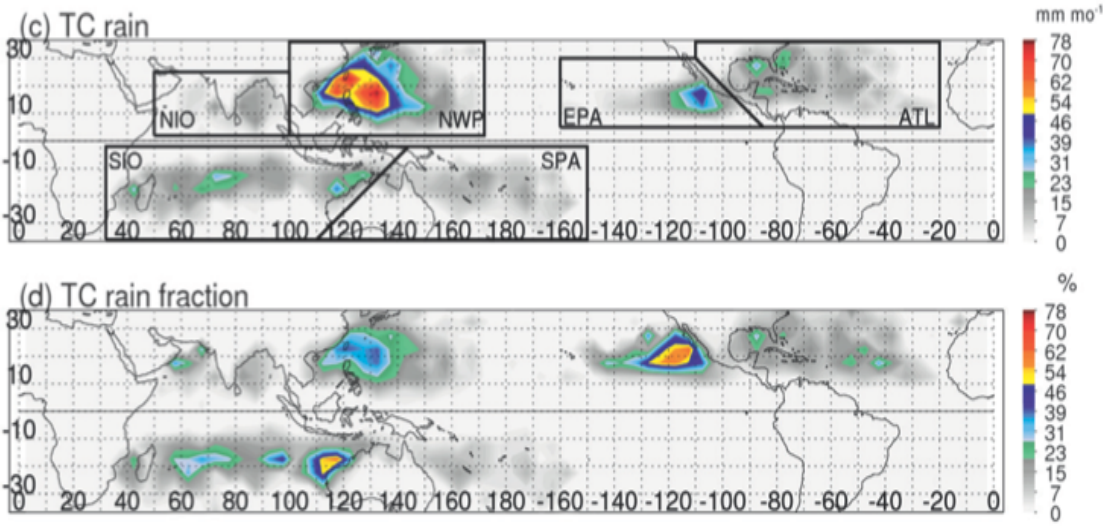

Figure 2.2. The 2A25 (c) TC rain, and (d) TC rain fraction based on 58 grid averages for the TC season (June–November for ATL, EPA, and NWP basins; May–June and October–January for the NIO basin) for the years of 1998–2000 and 2002–06 in the Northern Hemisphere and November–April for the years of 1998/99–2005/06 in the Southern Hemisphere. Borders of six basins (ATL, EPA, NWP, NIO, SIO, and SPA) are indicated in (c) (Source: Figure 5 in Jiang and Zipser, 2010).

Table 2.1: Basin-averaged TC rain and rain fraction contributed by TCs in hurricanes (Hur), tropical storms (TS), and tropical depressions (TD) for the same time period as in Figure 2.2 (Source: Table 3 in Jiang and Zipser, 2010).

Basin	Rain (mm month^{-1})			Rain fraction (%)		
	Hur	TS	TD	Hur	TS	TD
ATL	3.6	2.9	1.4	3.6	2.9	1.4
EPA	2.6	2.5	1.9	2.4	2.4	1.8
NWP	8.2	5.1	4.2	5.3	3.3	2.7
NIO	0.6	1.8	2.2	0.6	1.8	2.2
SIO	2.2	2.3	2.2	2.2	2.3	2.2
SPA	1.6	1.3	1.2	1.3	1.1	1.1

Strong relationships have been found between rainfall accumulation and TC intensity (Cerveny and Newman 2000). Generally, there is a positive correlation between the amount of TCP and TC intensity (Jiang and Zipser, 2010). In most ocean basins, mean TCP and TCP fraction for tropical storms are less than TCP caused by hurricanes, and greater than TCP from tropical depressions (Table 2.1). The Indian Ocean is the only basin where this is not the case. TC intensity and TCP are much greater in the NWP basin than in other ocean basins.

The results for specific ocean basins are in agreement with the global TCP studies. During the TC season, TCs contribute 7% of the total rainfall to the North Pacific (NP) (Rodgers et al. 2000). The locations with the greatest TCP are near the Baja California coast and Northeastern of the Philippine Islands (Rodgers et al. 2000). Both (Jiang and Zipser, 2010) and Rodgers et al. (2000) found similar results, even though they used different data sources.

Station-based TCP studies in the Western NP are in agreement with the satellite-based research (Kubota and Wang 2009; Rodgers et al. 2000). In particular, the western Pacific coast has higher monthly TCP than the central NP and Eastern NP during June to November. The higher frequency of TC activity in this region is primarily responsible for this.

2.4 Temporal Variation of TC Precipitation

2.4.1 Seasonal Variation

The seasonality of TCP varies in different ocean basins (Jiang and Zipser, 2010). In the Atlantic Ocean, both of the mean monthly TCP and the percentage of rainfall attributed to TCs is greatest in September. This agrees with Rogers et al. (2000). TCs in the Atlantic commonly form due to enhanced North African easterly wave disturbances in September. In October, the baroclinic-Intertropical Convergence Zone system causes more non-TC rain. Jiang and Zipser (2010) found that monthly TCP and TCP fraction also peaks in August-September in the eastern Pacific and western NP. However, Rogers et al. (2000), found that monthly TCP and TCP fraction was highest in the western NP within September-October. Total rainfall (TC and non-TC) peaks in the western NP in July to August. The lag between the maximum TCP and total rainfall is not obvious in central and eastern NP. The maximum TCP and TCP fraction occurs in July-August in the eastern Pacific. Both the maximum TCP and TCP fraction occur in May in the northern Indian Ocean, as well in March in the southern Indian Ocean.

2.4.2 Interannual Variations

Generally, the magnitude of the interannual variations in TCP in the North Atlantic is less than the NP. The primary reason is the lower TC frequency and intensity in the NAT (Rodgers et al. 2000; Rodgers et al. 2001). Inter-annual variability in the frequency and intensity of TC is influenced by many factors including sea level pressure (SLP), sea surface temperature (SST), wind shear, and tropospheric moisture (Gray 1984b; Shapiro and Goldenberg 1998; Lau et al. 2008). Toese factors are also directly or indirectly influenced by climate oscillations such as El Niño/Southern Oscillation (ENSO), North Atlantic Oscillation (NAO) and Quasi-Biennial Oscillation (QBO) (Gray 1984a; Kossin et al. 2010; Camargo and Sobel 2010). The relationship between TCP and teleconnections will be discussed in more detail in section 2.6.

2.4.3 Long-term Trends in TCP

Lau and Zhou (2012) examined trends in TCP over two decades (1988-1997 and 1998-2007) in both of the North Atlantic and NP. They detected an upward trend in TCP in the North Atlantic and a downward trend in the northwest Pacific. An increase in typhoon rainfall intensity since 2004 was found in Taiwan. This trend is due to more slow-moving TCs and a shift in the storm tracks (Chang et al. 2013). Also, increases in extreme rainfall attributed to TC have been found within different regions of the world, such as Korea and southern China (Kim et al. 2006, Wu et al. 2007). As the intensity of TCs increases, this tends to enhance rainfall rates, latent heat release, and the contribution from heavy rain to the total TC precipitation in the Western North Atlantic Ocean (Rodgers et al. 1994). TC-related extreme rainfall has increased in the United

States in recent decades (Knight and Davis 2009). The number of heavy rainfall events related to TC events exceeds the long-term mean. Even though only part of the U.S. is influenced by TCs, they account for about one third of the national annual extreme precipitation events (Kunkel et al. 2010). TCs contribute most to the extreme rainfall events along the east coast of the U.S. and Gulf of Mexico (Shepherd et al. 2007, Barlow 2011).

The precipitation rate in TCs may increase in a warming climate in future (Knutson et al. 2008; Gualdi et al. 2008). The projected overall increases in rainfall for the late 21st century (compared with present day) range from 3% to 37% (Knutson et al. 2010). However, the annual mean rainfall contributed to TC is still uncertain since changes in TC frequency are not well understood (Gualdi et al. 2008; Knutson et al. 2008).

2.5 TCs and Teleconnections

ENSO is thought as the most important driver of variations in TC frequency, intensity and TCP in the North Atlantic (Gray 1984a; Goldenberg and Shapiro 1996; Rodgers et al. 2001; Zhu et al. 2013). However, there are some other factors besides ENSO that also suppress or enhance TC activity in the NAT.

2.5.1 El Niño/Southern Oscillation

ENSO is the strongest and most well-known teleconnection. Past research demonstrated that ENSO influences TC activity on seasonal timescales (Gray 1984a; Landsea et al. 1999; Klotzbach and Gray, 2003; Kossin et al. 2010). Atlantic TC activity is decreased during El Niño years and enhanced during La Niña years. ENSO is also

associated with the frequency of landfalls in Golf of Mexico and the Caribbean (Landsea et al. 1999; Smith et al. 2007).

A number of past research have examined the relationship between ENSO and TCP. Jiang and Zipser (2010) found that TCP and TCP fraction increases (decreases) in the GMX, Western North Pacific, Eastern Pacific, western South Indian Ocean and southern of North India Ocean during El Niño (La Niña) years . However, TCP decreases in the majority NAT, coast regional of India, Southern Australia and some parts of the South China Sea during El Niño events. Rodgers et al. (2000) found that El Niño events suppress TCP in the North Atlantic mainly because of the enhanced upper-tropospheric winds and vertical wind shear. Zhu et al. (2013) found that ENSO was the most significant factor that controlled TCP in Texas.

2.5.2 North Atlantic Oscillation

The NAO is a prominent teleconnection patterns for North Atlantic in all seasons. It is defined as the sea level pressure difference between the Icelandic Low and the Azores High (Jones et al. 1997). The positive phase of the NAO is related to a weaker Icelandic low and a higher than normal subtropical high. On the other hand, the negative phase of the NAO is associated with the opposite conditions and a weaker pressure gradient in the North Atlantic. Past studies have demonstrated that the NAO can influence the frequency of Atlantic TCs as well as the frequency of landfalls in the U.S. (Elsner and Jagger 2006; Sabbatelli and Mann 2007; Kossin et al. 2010). For example, the number of TC that make landfall in the U.S. tends to be above mean when NAO is in the negative phase (Elsner and Jagger 2006). NAO modifies TC tracks in North Atlantic.

The May to June NAO influences the occurrence of "straight moving" hurricanes and more straight moving hurricanes occur when the NAO is negative. Straight moving hurricanes tend to increase TC activity in the Caribbean and south of 35°N North America, while recurving hurricanes tend to increase TC activity north of 35°N (Elsner 2003; Kossin et al. 2010) (Figure 2.3). The negative NAO is also associated with anomalously low sea level pressure, which is correlated with an increase in Atlantic TC genesis (Knaff 1997). Sabbatelli and Mann (2007) found that NAO influence annual TC counts in the Atlantic. NAO was also a significant variable in the multiple linear regression models that were developed to predict TCP in Texas (Zhu et al. 2013).

2.5.3. Atlantic Meridional Mode

The Atlantic Meridional Mode (AMM) also influences TC activity in the North Atlantic. The AMM describes the major pattern of coupled ocean atmosphere interaction between low-level winds and sea surface temperature (Chiang and Vimont 2004). It is related to the Atlantic Multidecadal Oscillation (AMO). AMO impacts multi-decadal variability of NAT TC activity and its impacts on seasonal TC activity are manifested through AMM (Vimont and Kossin 2007). On a decadal timescale, AMM and AMO have a similar relationship with large-scale climatic variables. That is, AMO is the excitation of decadal AMM (Vimont and Kossin 2007). On the contrary, AMM is related to both of decadal and inter-annual fluctuation of TC activities. AMM is associated with TC intensity (Vimont and Kossin 2007), tropical cyclogenesis (Kossin et al. 2010) and TC tracks (Xie et al. 2005). AMO is strongly correlated with TCP volume as well as TCP area in the eastern U.S., but it has a negative correlation with non-TC rainfall

(Nogueira and Keim 2010). This study will only investigate the relationship between AMM and TCP.

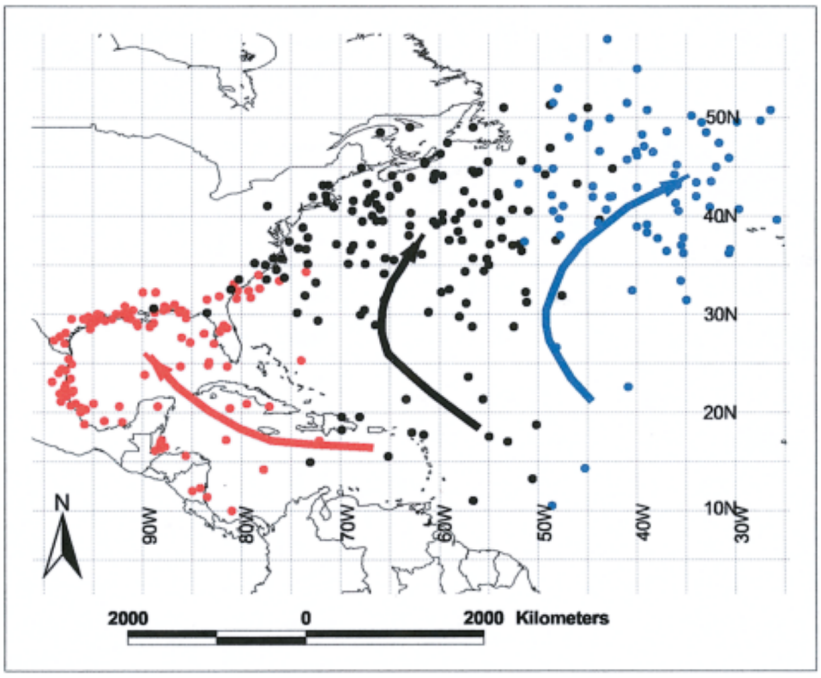

Figure 2.3 Terminal locations of hurricanes over the period 1944–2000 grouped by track type. Track type is determined using a k-means cluster analysis. Here k = 3. The red circles and path represent straight-moving hurricanes. The black and blue circles and paths represent recurving hurricanes. Track paths are based on the average positions of the hurricanes at initial hurricane intensity, maximum hurricane intensity, and final hurricane intensity. Data are from the U.S. National Hurricane Center. (Source: Figure 1 in Elsner, 2003).

2.5.4 Quasi-Biennial Oscillation

The stratospheric quasi-biennial oscillation (QBO) represents shifts in tropical stratospheric winds. Past research found that TC activity tends to increase (decrease) when is in the westerly (easterly) QBO phase (Gray 1984a, 1984b; Shapiro 1989). The correlation between QBO and TC in the Atlantic is stronger than other ocean basins. Actually, the relationship between QBO and TC activity was relatively strong between the 1950s to 1980s, but got weaker after the 1980s and it is now not statistically significant (Camargo and Sobel 2010). The physical mechanism of the correlation between QBO and TC activity is still a matter of debate.

CHAPTER III

DATA AND METHODS

3.1 TRMM Data

This thesis uses the TRMM tropical cyclone precipitation feature (TCPF) database (Jiang et al., 2011). It is a subset of University of Utah (UU) TRMM precipitation feature (PF) database. Jiang et al. (2011) create the TCPF from the TRMM 3B42 data. TRMM 3B42 is a multi-satellite rainfall product that combines microwave and infrared radiation (IR) (Huffman et al. 2007). The microwave data collected from the satellite including: TRMM Microwave Imager (TMI), Special Sensor Microwave Imager (SSM/I), Advanced Microwave Scanning Radiometer (AMSR), Advanced Microwave Sounding Unit (AMSU) (Huffman et al. 2007). The IR data comes from the international constellation of geosynchronous earth orbit (GEO) satellites. TRMM 3B42 is a relatively high spatial resolution (0.25° x 0.25°) and temporal resolution (3-hourly) rainfall product. To define TCP, all 3B42 pixels within 500 kilometers radius of the tropical cyclone center of circulation are attributed to the TC. This thesis uses 14 years (1998-2011) of TCP data in North Atlantic from the 3B42 PF dataset. This study calculates the accumulated TC rainfall for each year by summing the rainfall attributed to TC events in each grid.

3.2 Total Rainfall

This thesis also quantifies the total annual and seasonal rainfall, which includes all TC and non-TC rainfall. These data are from TRMM 3B43 Version 7. Similar with TRMM 3B42, 3B43 is also a multi-satellite rainfall product. The only difference

between the two data sets is the temporal resolution because TRMM 3B43 is a monthly product.

3.3 TC Metrics

TC features such as TC intensity and TC frequency are used in the study. These two TC characteristics are most commonly used in the past research for evaluating the TC activity. Data on TC activity are acquired from the Tropical Prediction Center (TPC, formerly the National Hurricane Center)/National Oceanic and Atmospheric Administration (NOAA) for the Atlantic basin (Jarvinen et al. 1984). The Accumulated Cyclone Energy (ACE) index was used because it is a comprehensive measure of hurricane intensity. ACE index can reflect wind energy and it is calculated by summing the square of the maximum wind speed of active tropical storm every 6 hours (Bell et al. 2000). We have downloaded the time series of the index from the hurricane database (HURDAT) (www.aoml.noaa.gov/hrd/hurdat/comparison_table.html).

3.4 Teleconnections

As shown in Chapter 2, El Niño/Southern Oscillation, North Atlantic Oscillation, Atlantic Meridional Mode, and Quasi-Biennial Oscillation are four of the most significant controls of TC activity in the North Atlantic. Thus, these four teleconnections will be considered in my study. Numerous indices have been used to represent ENSO, such as Niño 3.4, Southern Oscillation Index (SOI), and the Multivariate ENSO Index (MEI). The MEI will be used in this thesis because it integrates information from the other indices (www.cdc.noaa.gov/people/klaus.wolter/MEI/table.htm). The NAO index

is calculated with the sea level pressure difference between Gibraltar and Reykjavik, Iceland (Jones et al. 1997) and it is available from the Climate Research Unit (http://www.cru.uea.ac.uk/~timo/datapages/naoi.htm). The monthly AMM index used here is from the NOAA Earth System Research Laboratory (http://www.esrl.noaa.gov/psd/data/timeseries/monthly/AMM/). The AMM index is calculated by Chiang and Vimont (2004). The AMM is defined by using Maximum Covariance Analysis (MCA) to meridional SST gradient and low level (10 m) winds field over the region (74°W-15°E, 21°S-32°N). Following Chiang and Vimont (2004), this study applied the SST expansion coefficient from the MCA. The University of Berlin have developed the QBO dataset and it is available online at: (http://www.geo.fuberlin.de/en/met/ag/strat/produkte/qbo/index.html).

3.5 Study Area

In this study, we focus on the North Atlantic, a geographical domain delineated by 100°W to 2.5°W, 0°N to 50°N. Based on Chapter 2, there are major differences between TC activity within the North Atlantic, thus three sub-basins was identified: Gulf of Mexico (GMX), Caribbean (CAR), and East Coast (ECO)(Figure 3.1). The boundaries of spatial domains are shown in Table 3.1. These sub-basins were defined following Zhu et al. (2013).

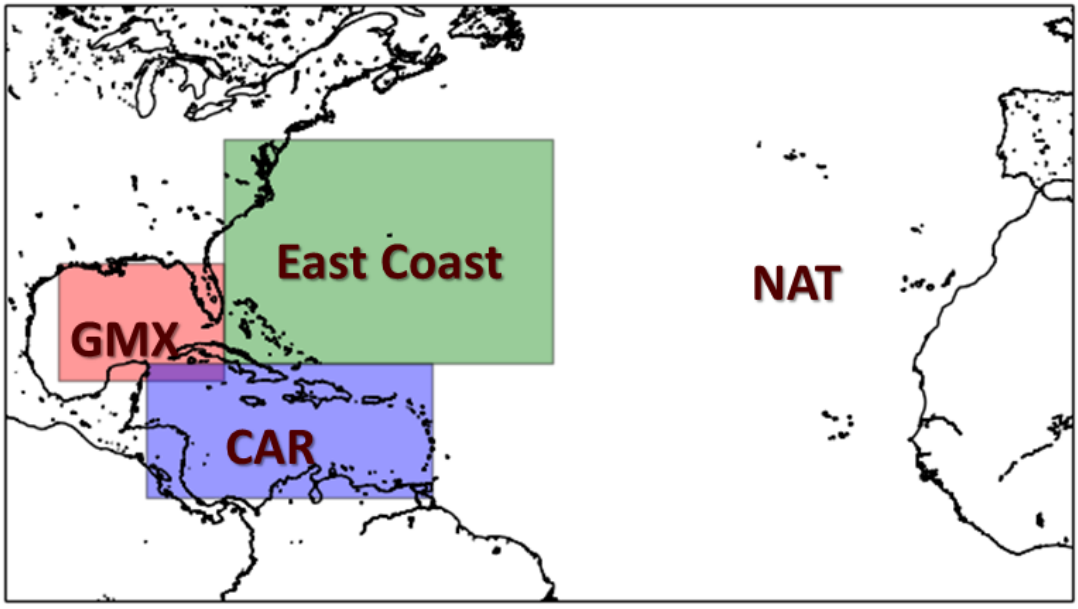

Figure 3.1 Spatial domains used in the research

Table 3.1 Description of study area

Abbreviation	Description
NAT	North Atlantic Ocean (100°W to 2.5°W, 0°N to 50°N)
GMX	Gulf of Mexico (95°W to 85°W, 20°N to 30°N)
CAR	Caribbean (87°W to 61°W, 9.5°N to 21.5°N)
ECO	East Coast (80°W to 50°W, 21.5°N to 40°N)

3.6 Methods

3.6.1 Spatial Variations in TCP in North Atlantic and Sub-basins

Accumulated TCP is calculated by summing up all storms in a given year. Mean annual TCP is determined be summing TCP in each grid cell and dividing by the number of the years. An analysis of mean TCP will be completed and summary statistics will be calculated to identify the variability of TCP. The analysis will be done for the entire North Atlantic as well as for each of the sub-basins.

3.6.2 Spatial Distribution of Mean Annual Rainfall and TCP Contribution

Monthly TRMM (3B43) data is applied to calculate the average annual and mean seasonal rainfall in the North Atlantic. The contribution (ratio) of rainfall attributed to TCs is calculated for each grid cell. The results of this analysis will be compared to previous studies.

3.6.3 Monthly and Seasonal Variations in TCP

Seasonal variation in TCP is examined based on the accumulated rainfall volume. Rainfall volume combines both rainfall depth and rainfall area for each year. The TCP volume in every grid cell in the study region was summed to calculated the TCP volume. The causes of the monthly and seasonal variations in TCP will be explored by creating statistical models that examine the relationships between TC intensity (ACE index), TC frequency (TC counts) and TCP volume. Trends in TCP fraction and TCP volume will also be examined.

3.6.4 TCP and Teleconnections

The relationship between TCP and NAO, ENSO, QBO and AMM will be examined by constructing statistical models. The dependent variables will be annual and monthly TCP and TCP volume. Regression models will be used to identify the relationship between teleconnections and TCP. The impact of teleconnections on TCP will also be assessed using composite analysis. TCP in years with high/low indices will be calculated and the differences in TCP between years with high and low indices will be mapped. The spatial patterns can be used to help explain the impacts of teleconnections on TC frequency, intensity, and track.

CHAPTER IV

TEMPORAL AND SPATIAL VARIATIONS IN TCP

4.1 Spatial Variation of TC Precipitation

Figure 4.1 shows annual TCP between 1998 and 2011. Annual TCP varies substantially from year to year. Both the TCP area and location of TCP maxima varied from year to year. The shape of the TCP region corresponds with the tropical cyclone track. In some years, such as 1998, 2005, 2010 and 2011, TCP is dispersed in the NAT. On the contrary, TCP is concentrated in 2000, 2002, 2006, 2007, and 2009. TCP is relatively high in 1999 and 2005 and it is relatively low in 2002, 2006, and 2009. Annual mean TCP is greater than 450 mm per year in eastern GMX and northern CAR. The TC was most active in the historical record in 2005 hurricane season and it resulted in nearly 1700 deaths, including 1500 in the U.S. from Hurricane Katrina (Beven II et al. 2008). Four hurricanes reached Category 5 in 2005, while no hurricane reached Category 5 in 2002 (Pasch et al. 2004; Beven II et al. 2008).

During the period of 1998 and 2011, the North Atlantic experienced an average of 14.85 TCs every year. The number of TCs varied from 28 in 2005 to only 6 in 2002. Figure 4.1 displays that there is an obvious relationship between annual TCP and the number of TC events. For example, 2005 had much more TCP compared to other years.

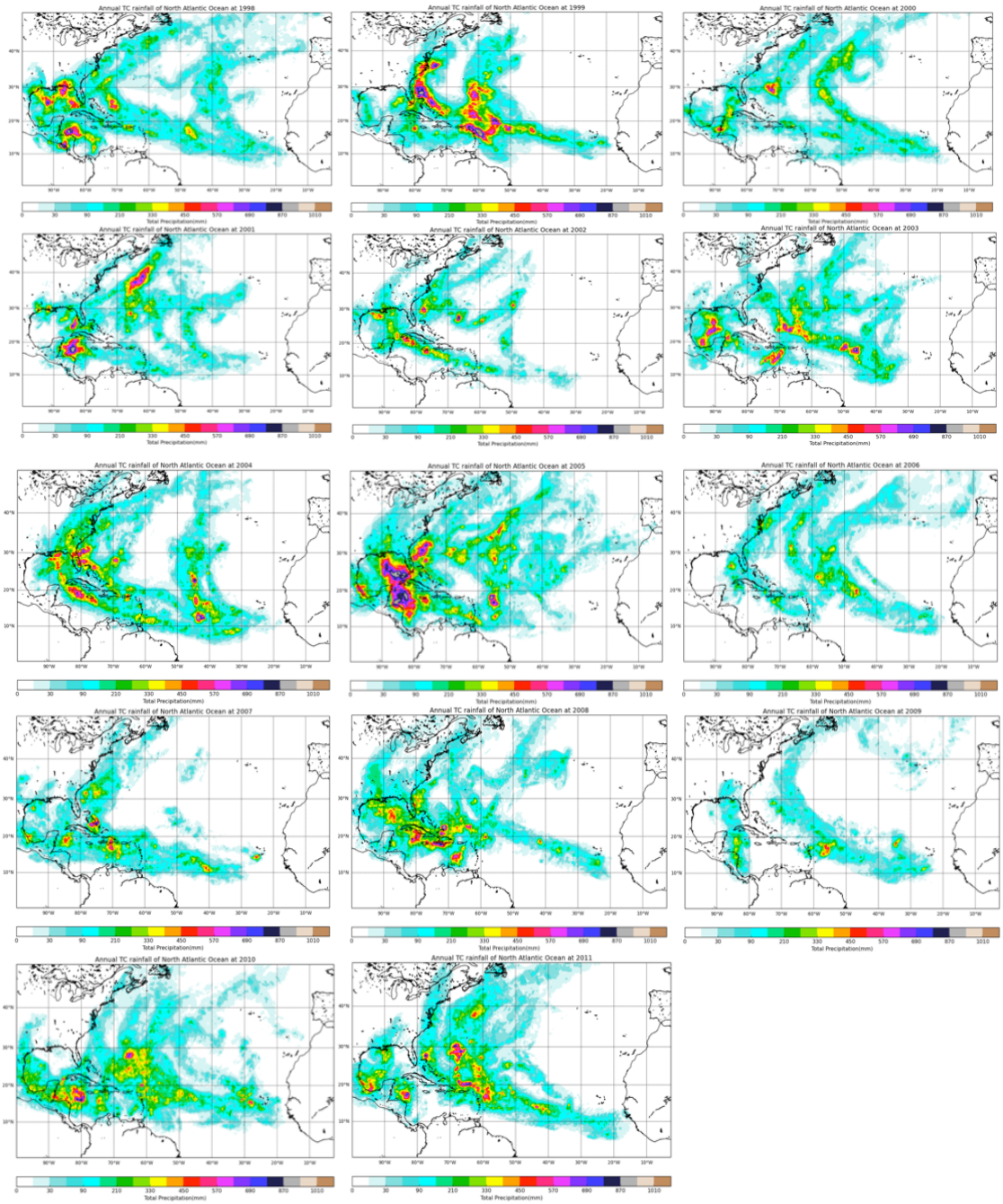

Figure 4.1. Annual TCP (mm) for 1998 to 2011.

Figure 4.2 shows the mean annual TCP in the NAT. It is evident that there is a substantial gradient in TCP. TCP is generally higher in the west and central North Atlantic and very little TCP occurs in the eastern NAT and equatorward of 15°N latitude. There are several regions that have relatively high mean annual TCP including off the east coast of U.S., eastern Gulf of Mexico, northern Caribbean, as well as Bermuda and a band that extends along 20°N into the central North Atlantic. The highest TC rainfall between 1998 and 2011 was found in the Gulf of Honduras (15°N, 88°W) and it has mean annual TCP of 333 mm. Mean annual TCP for the entire NAT is 79 mm.

Figure 4.2 also shows the zonal mean TCP in the North Atlantic. TCP gradually increases as one moves from 50°N towards the equator and a maximum at about 18°N, before decreasing equatorward of this latitude.

Rodgers et al. (2001) used SSM/I to calculate mean monthly TCP in the North Atlantic Ocean (Figure 4.3). Although they used a different data source and time period, the general spatial pattern of TCP and the location of some of the TCP maxima are similar. Rodgers et al. (2001) also found that TCP was higher along the east coast of the U.S., east of the Gulf of Mexico, northern Caribbean, Bermuda and a band along 18°N. The primary difference between this TRMM-based analysis and the findings of Rodgers et al. (2001) is the position of the TCP maxima. This is not surprising given that the studies had different time periods and TCP maxima are strongly influenced by individual TCs.

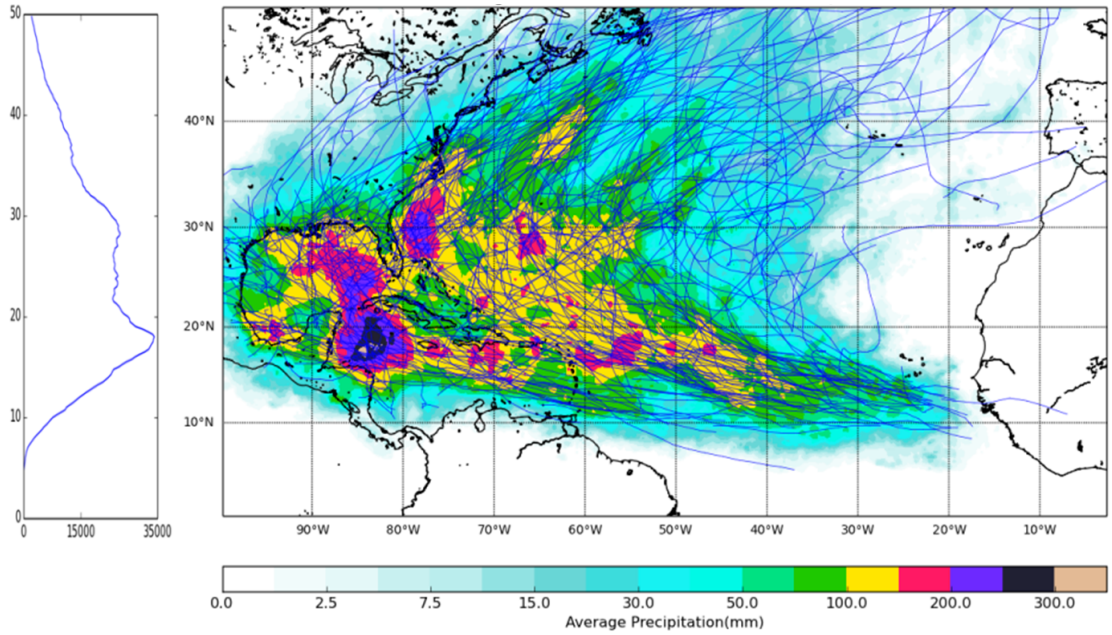

Figure 4.2. Mean annual TCP (mm) in the North Atlantic (1998-2011).

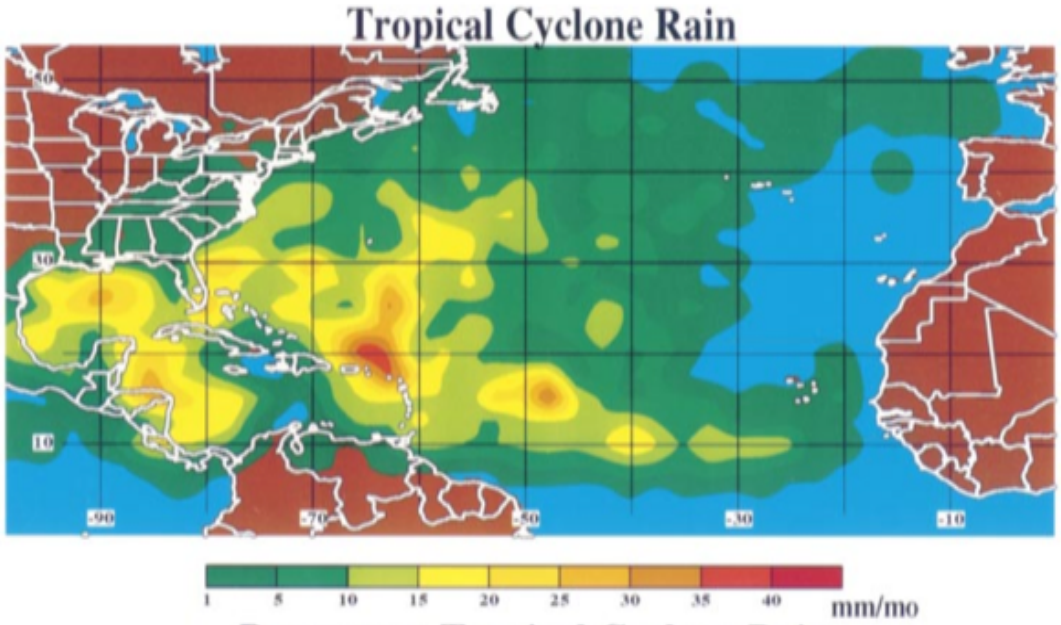

Figure 4.3. A plan view showing the SSM/I-derived mean monthly North Atlantic rainfall amounts (mm per month) contributed by tropical cyclones for Jul–Nov 1987, Jun–Nov 1988–89, and 1991–98 (a 65-month period). Brown and blue backgrounds designate, respectively, non-raining land and ocean areas. (Source: Figure 3 in Rodgers et al. 2001)

4.2 TCP Distribution in Sub-basins

Most of the Gulf of Mexico has a relatively high mean annual TCP (Figure 4.4). The areal mean for the GMX is 140 mm per year. This is the highest among all the sub-basins. The eastern half of the GMX receives more TCP than the western half. TCP also decreases from south to north and it tends to be lower in the land than over the oceanic region. The spatial distribution of TCP in this region is similar to a station-based assessment of TCP in Texas (Zhu et al. 2013).

Mean annual TCP is 116 mm in CAR. The spatial distribution of TCP is very heterogeneous and most of the TCP is concentrated in the northern part of the CAR region (Figure 4.5). The highest TCP locates in northwest of CAR. TC rainfall decreases from north to the equator. There is little precipitation south of 10°N due to the fact that TCs rarely passing through this region.

Mean annual TCP is 116 mm in CAR. The spatial distribution of TCP is very heterogeneous and most of the TCP is concentrated in the northern part of the CAR (Figure 4.5).

Mean annual TCP in the ECO is 101 mm per year. The highest TCP occurs off the coast of Florida (Figure 4.6). TCP in the southern and western ECO are higher than the northern and eastern ECO.

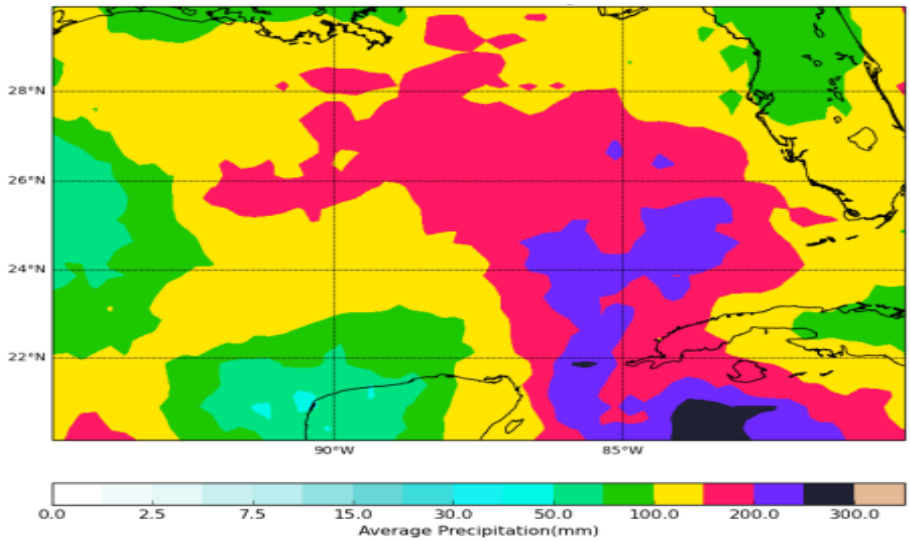

Figure 4.4 Mean annual TCP (mm) in GMX (1998-2011).

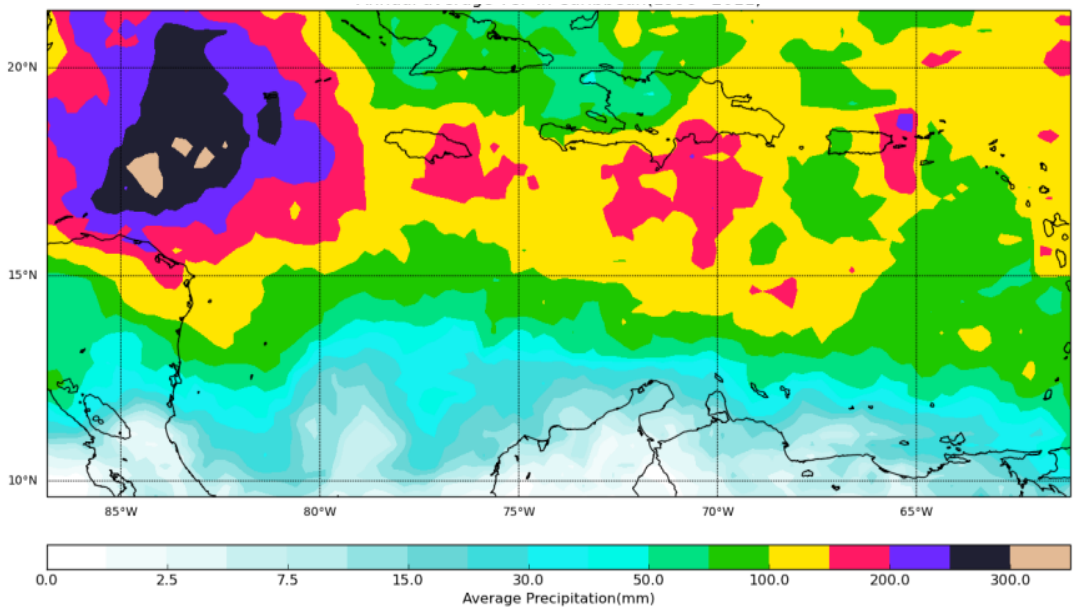

Figure 4.5. Mean annual TCP (mm) in CAR (1998-2011).

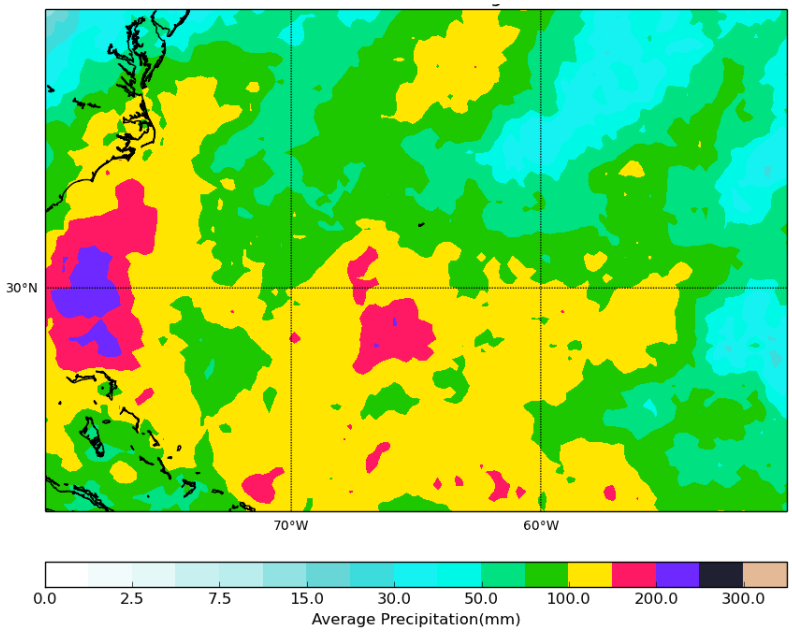

Figure 4.6. Mean annual TCP (mm) in ECO (1998-2011).

4.3 TCP Ratio

TRMM 3B43 data was used to calculate seasonal precipitation in the North Atlantic (Figure 4.7). This is based on using a hurricane season from June to November (JJSAON). Compared with TCP, the variability of total seasonal precipitation (all TC and non-TC precipitation) is not as obvious. Figure 4.8 shows the mean seasonal precipitation in the North Atlantic. The highest value (5956 mm/season) appears off the west coast of Colombia. The mean seasonal rainfall is 825 mm per season for the entire North Atlantic Ocean.

Similar to Rodgers et al. (2001), the highest rainfall amount corresponds with the Hadley Circulation's ascending branch. The highest seasonal rainfall off the ECO of the U.S. corresponds with the average position of the active baroclinic zone. The regions with relatively low seasonal rainfall in the subtropics, northwestern Africa, and the southeastern U.S. are related to the Hadley Circulation's descending branch.

The percentage of rainfall attributed to TCs is shown in Figure 4.9. The region where TCs make the greatest contribution are located in the western and central portions of the NAT between 10°N to 20°N. The highest percentage of rainfall attributed to TCs during the period is 34%. Compared with the oceanic area, there is a lower percentage of TCP over land. TCs account for about 10% of the rainfall in the Caribbean Islands and southeastern U.S.. These are the land areas with the highest TCP contribution attributed to TCs.

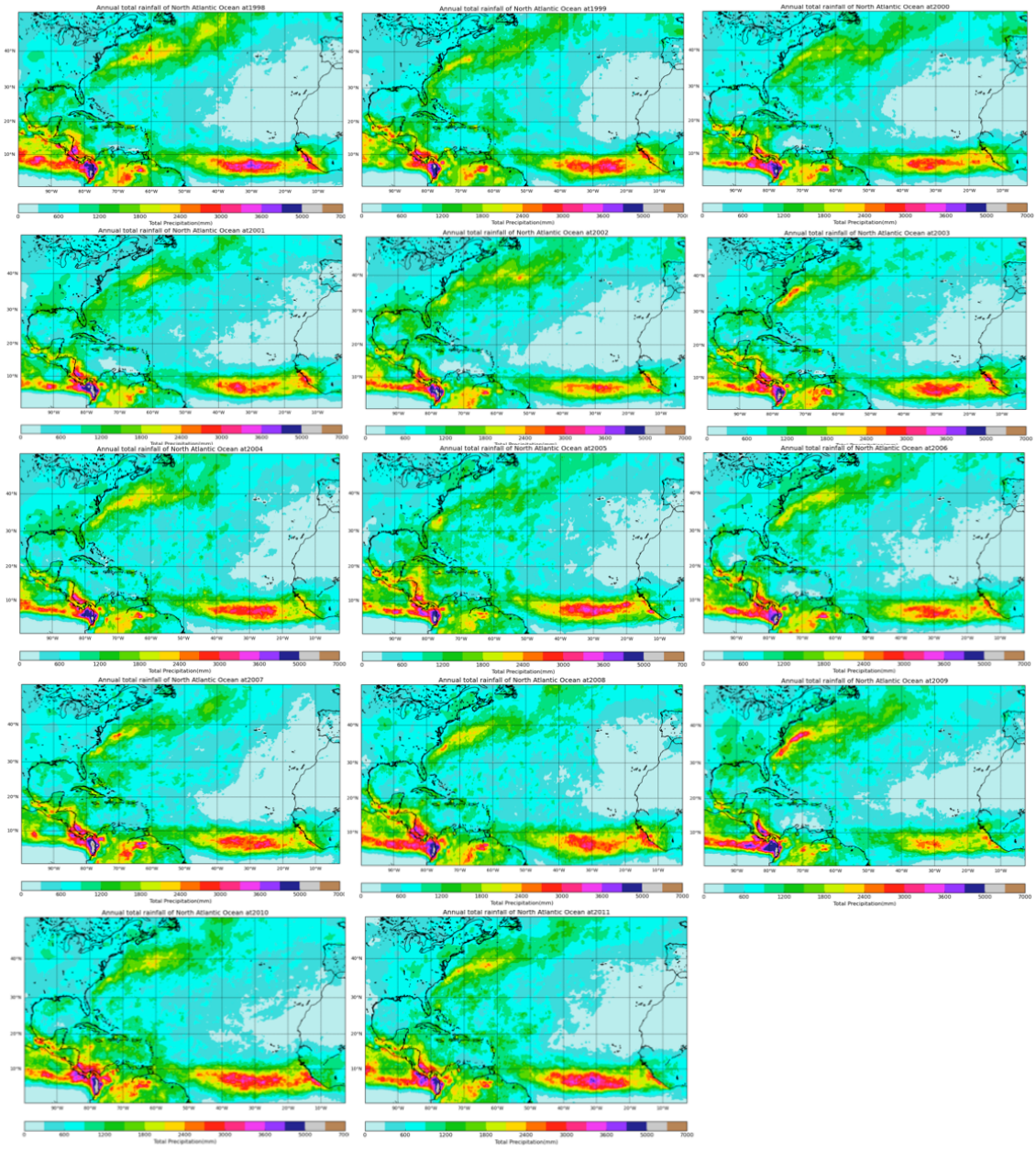

Figure 4.7 Interannual variations in seasonal (JJSAON) precipitation (mm) from 1998 to 2011.

A comparison of Figures 4.2, 4.8 and 4.9 reveals that the region with the most TCP is a bit of northward of the region with the highest total precipitation. This result is similar to what Rodgers et al. (2000) found in the NP. In NAT, TCP contributed the most rainfall in the west of ITCZ and north of subtopics, which is a region with relatively low total rainfall. Most of TC recurved and intensified in the region. The highest rainfall totals are concentrated in the areas between equator and 10°N latitude, however there is very little TC activity within this region because of the weak Coriolis. The TCP contribution is nearly 0% equatorward of 10°N latitude. Compared with other TCP maxima, the TCP contribution along the ECO of the United State. is not higher than other regions. This is primarily because the total precipitation in this region is also relatively high. In contrast, some regions receive a lot of TCP but have relatively low total precipitation, and so TCP plays a more significant role in these regions. For example, in the Gulf of Honduras the mean total precipitation in each hurricane season is less than 1200 mm and TCP is about 300 mm.

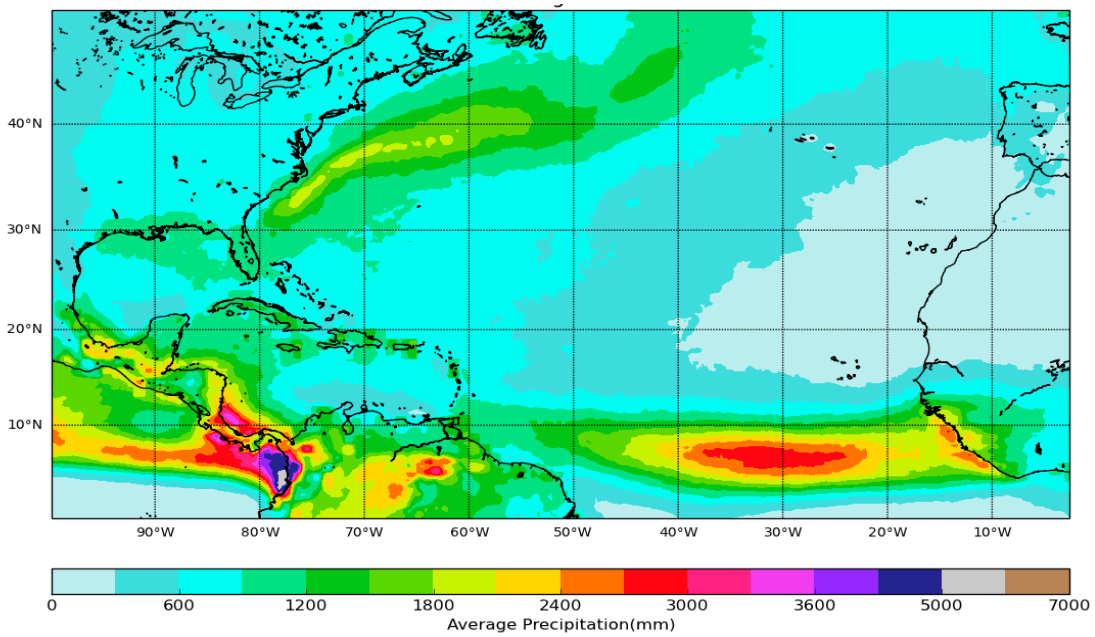

Figure 4.8. Mean annual precipitation (mm) over NAT (1998-2011).

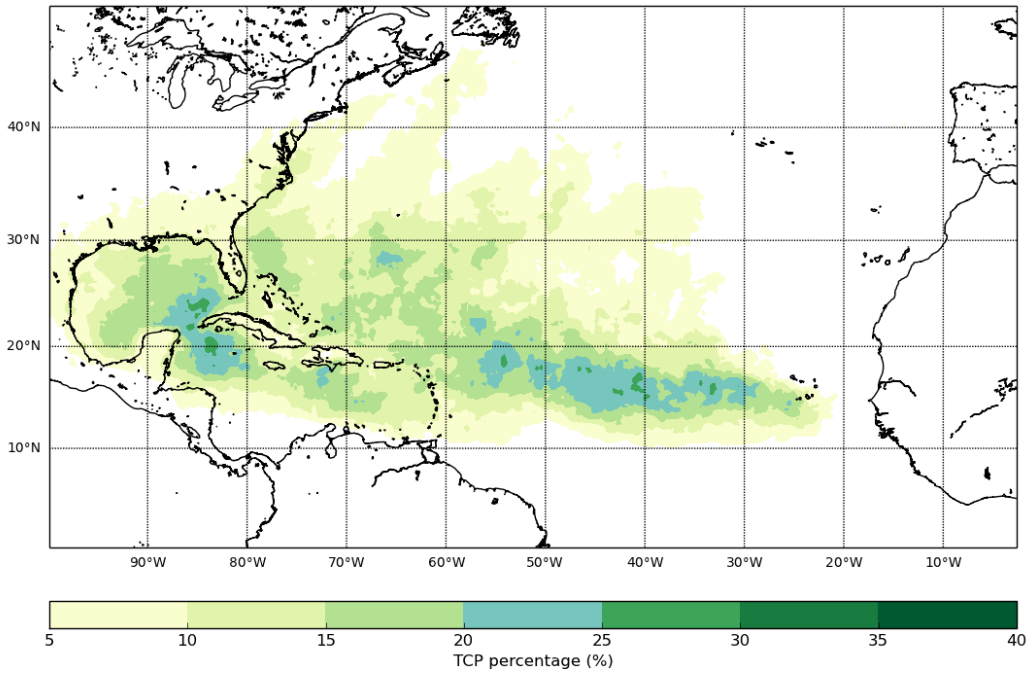

Figure 4.9. Mean percentage of precipitation attributed to TCs in the NAT (1998-2011).

Rodgers et al. (2001) shows similar results for the percentage of TCP (Figure 4.10). However, there are some differences between the two studies. Generally, both show that the highest TCP percentages occurred between 10ºN and 30ºN and the TCP percentage decreases from ocean to the land. Compared with the high TCP percentage shown near the Caribbean islands in Figure 4.9, the TCP percentage in Figure 4.10 does not match in this region. The TCP percentage maxima in the southeastern of Gulf of Mexico also does not appear in Rodgers et al. (2001). There is a region of high TCP percentages (>25%) in the NAT between 10ºN and 20ºN (Figure 4.9). Rodgers et al. (2001) shows relatively high TCP percentages in that region, but the percentages are 5-10% lower than my result.

4.4 Temporal Variations of TCP

4.4.1 Seasonal TCP

Seasonal variations in TCP were examined using accumulated annual rainfall volume. The volume combines both rainfall depth and rainfall area and it can be directly compared between hurricane seasons. The formula for TC volume is:

$$V_{TCP} = \Sigma\, RR_{TCP} \times Hours_{year} \times Area_{grid}$$

where V_{TCP} is accumulated volume of TCP in each year. RR_{TCP} is TRMM-based rain rate (mm/h) within a 2.5° latitudinal x 2.5° longitudinal grid. $Hours_{year}$ is the number of hours in a hurricane season per year and $Area_{grid}$ is the area of each 2.5° latitudinal–longitudinal grid.

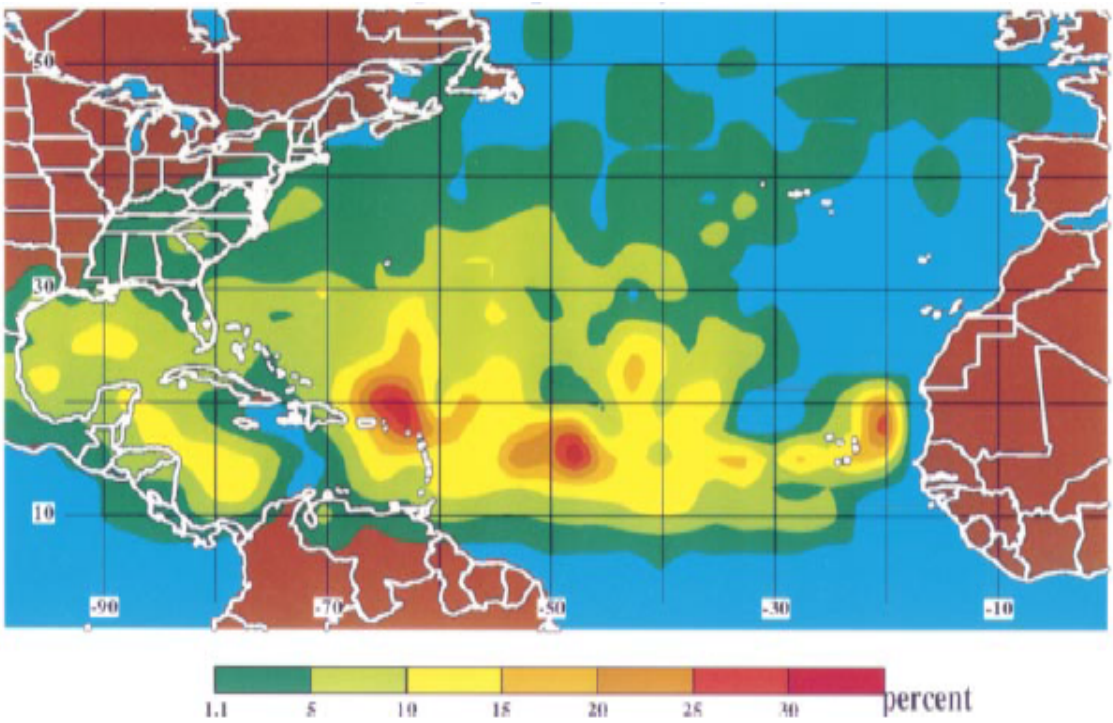

Figure 4.10. Same as Figure 4.3, except it shows the fraction of tropical cyclone rainfall (percentage) (Source: Figure 3 in Rodgers et al., 2001).

The annual TCP volume is shown in Figure 4.11a. Generally, there is no statistical significant trend in the TCP volume between 1998 and 2011(Figure 4.11b), but there are significant interannual variations. TCP volume reaches a maximum in 2005, which is the year when there were 28 TCs in the North Atlantic. There is obvious positive correlation between TC frequency and TCP volume (P-value < 0.05). Most of the variation (~60%) in TCP volume can be attributed to interannual variations in TC frequency (Figure 4.11c). However, there are some years that are outliers. For example, there were fewer TCs in 2002 than in 2009, however TCP volume in 2002 is greater than TC rainfall in the year of 2009. Therefore, more TCs do not necessarily produce more TCP because TCs are complex systems and it is difficult to identify all of the factors that cause variations in TCP.

Figure 4.12 shows that a significant positive correlation between TCP and TC intensity was found (as represented by ACE). Seasonal TCP and ACE index are highly correlated ($R^2 = 0.90$) (Figure 4.12b).

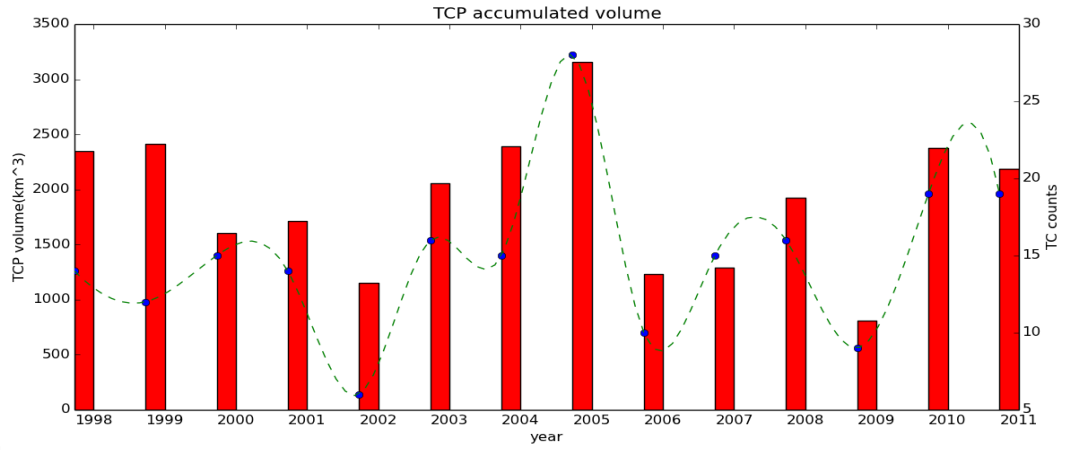

(a)

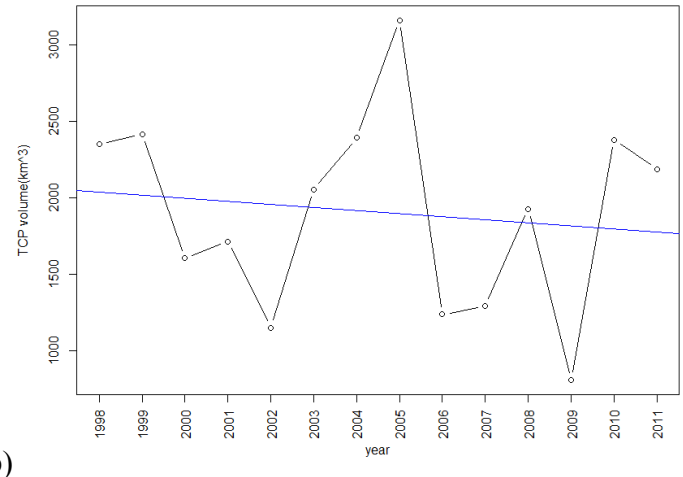

(b)

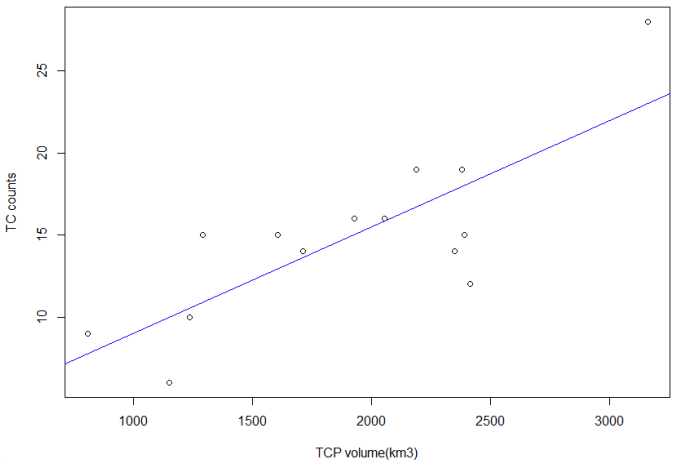

(c)

Figure 4.11 (a) Seasonal TCP volume (km3) (red bar) and TC count (green line) in the North Atlantic, (b) Time series of annual TCP volume, Blue line is fitted trend line (R2 = 0.02, P-value = 0.65), and (c) Scatter plot of TCP volume and TC count (R^2= 0.60).

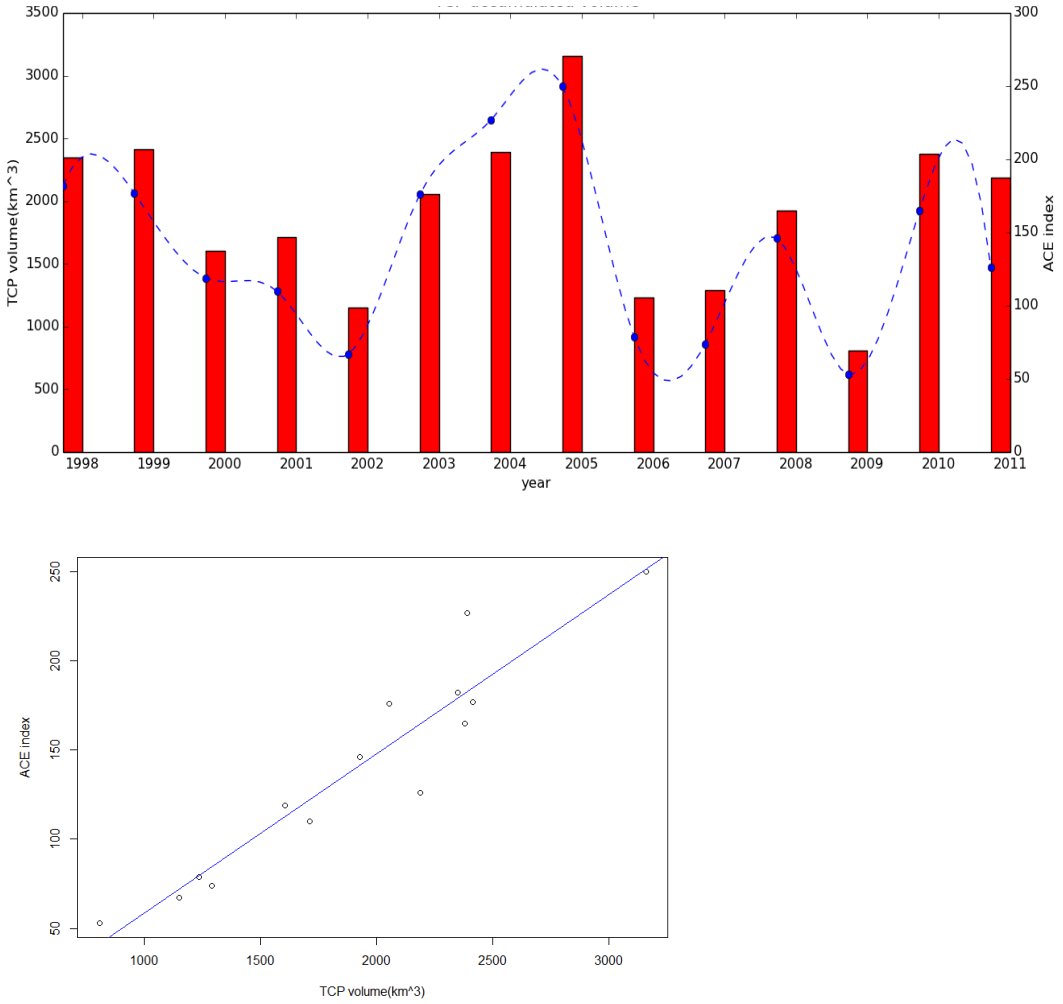

Figure 4.12 (a) Seasonal TCP volume (km^3) (red bar) and ACE index (blue line) in the North Atlantic, (b) Scatter plot of TCP volume (km^3) and ACE index. The best-fit line is shown in blue.

4.4.2 Trend in TCP and TCP Fraction

TCP fraction was calculated based on the following equation:

$$\text{TCP fraction} = V_{TCP}/V_{TP}$$

V_{TCP} is accumulated volume of TCP in each year, which is calculated before. V_{TP} is accumulated volume of Total precipitation in each year. It was calculated by similar method with V_{TCP}. The difference is only grid cell with TCP greater than 0 mm was counted in the accumulated volume. This method will improve the estimate of TCP fraction by excluding some locations that are outside the NAT, such as the Pacific Ocean near Colombia (Figure 4.8).

The temporal variations in total rainfall volume and TCP fraction are shown in Figures 4.13 and 4.14. Compared with TCP volume, total rainfall volume does not vary much between 1998 and 2011. TCP fraction is greatest in 2005, nearly 9%. While in 2009, TCs contributed less than 3% of precipitation in the North Atlantic. The time series of TCP fraction and total rainfall are shown in Figure 4.15. There is not a statistically significant trend in TCP fraction in the NAT between 1998 and 2011. Although the total rainfall has increased over the period, the trend is not statistically significant.

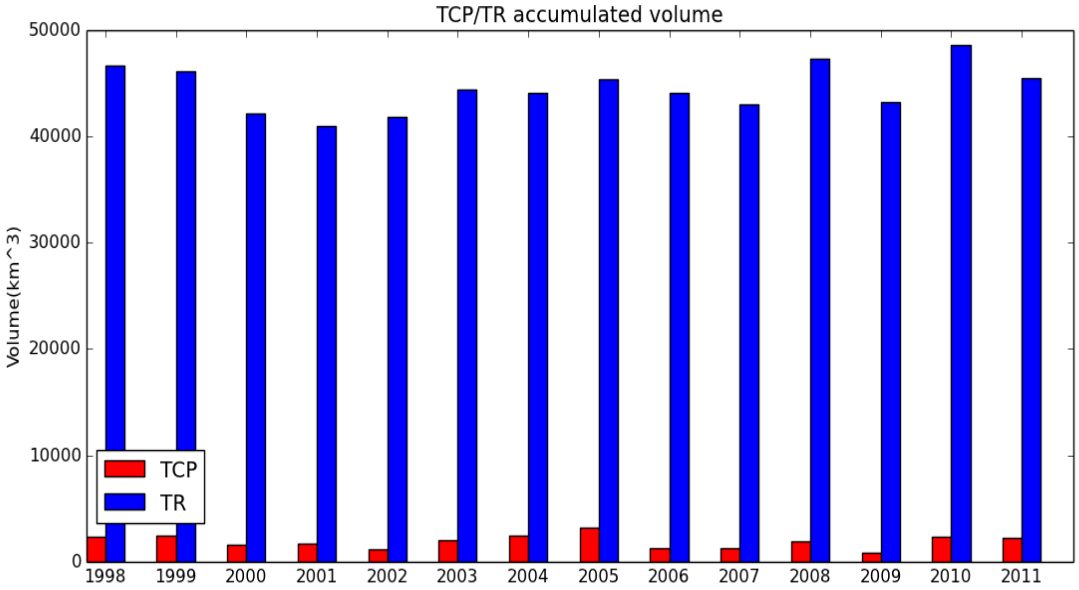

Figure 4.13. Seasonal TCP and total rainfall volume (km^3) in the North Atlantic

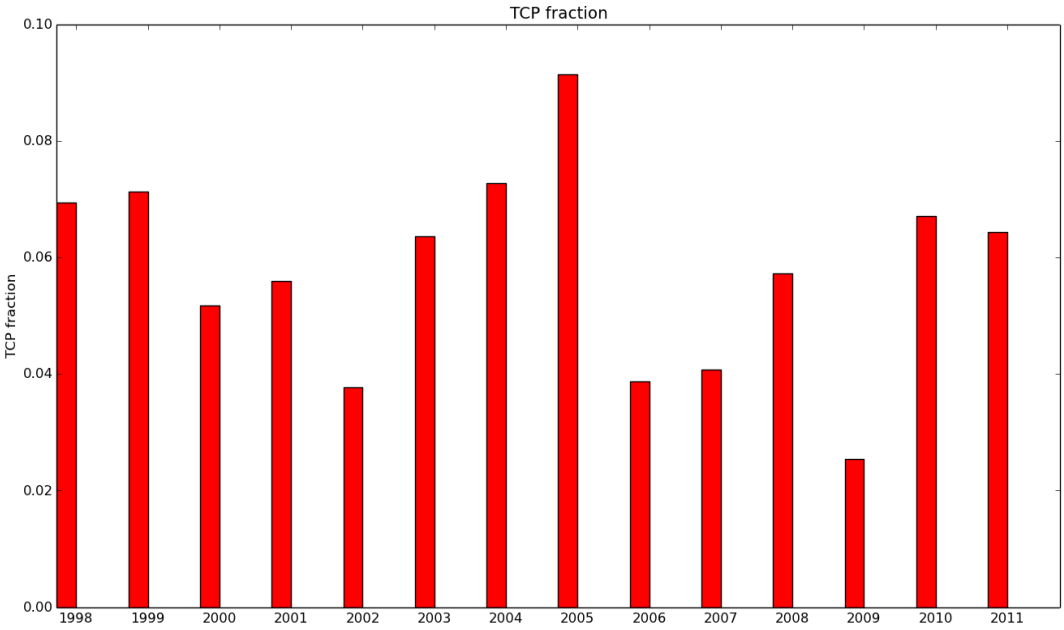

Figure 4.14. Seasonal fraction of TC rainfall in the North Atlantic

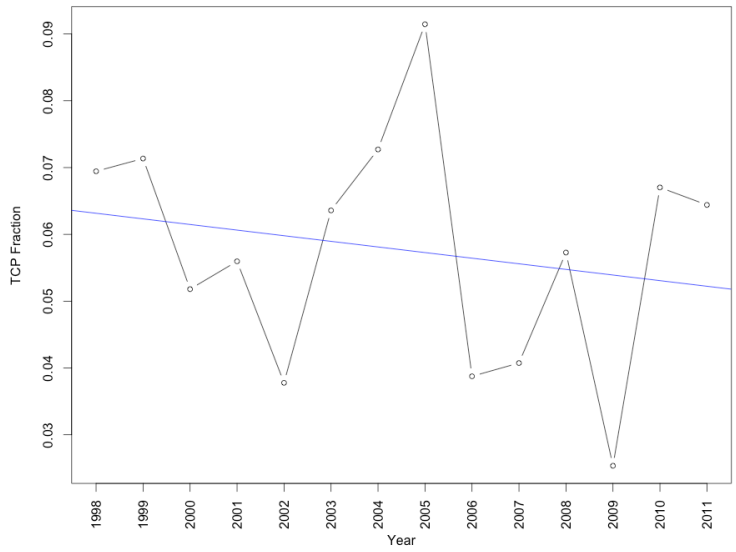

(a)

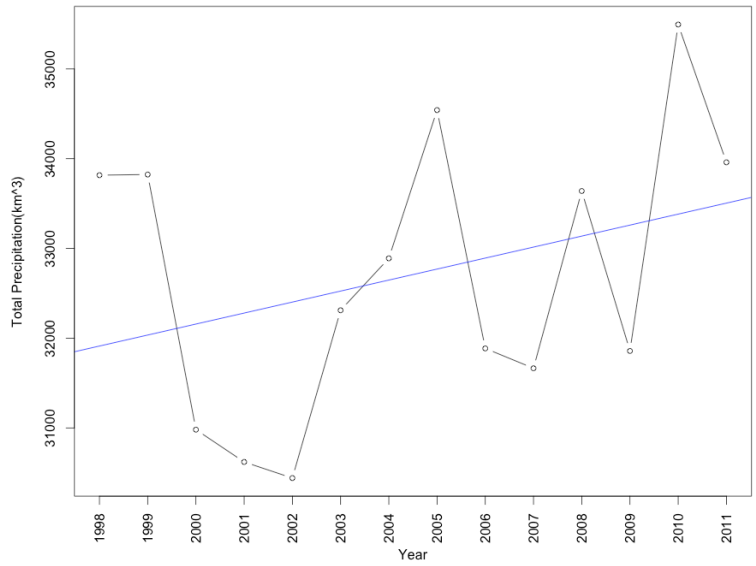

(b)

Figure 4.15. (a) Time series of annual TCP fraction. Blue line is fitted trend line (R^2 = 0.04, P-value = 0.49). (b) Time series of annual total rainfall (km^3). Blue line is fitted trend line (R^2 = 0.11, P-value = 0.25).

4.5 Summary and Conclusion

TCP is an important contributor to major rainfall events (Prat and Nelson 2013). A TC precipitation climatology was developed for the NAT and its sub-basins. Fourteen years of TRMM data were used to calculate TCP and total rainfall. The high-resolution TRMM data provide highly-resolved estimates of the spatial patterns of TCP in the North Atlantic. Generally, the spatial pattern of TCP agrees with the past research (Jiang and Zipser 2010, Rodgers et al. 2001). TCs contributed an average of 76 mm of precipitation per year in the North Atlantic. This varied from 140 mm per year in the Gulf of Mexico, 116 mm per year in the Caribbean and 101 mm per year for the East Coast region of the U.S. The Gulf of Mexico receives more TCP than any of the other sub-basins. Generally, the areas with higher mean annual TCP correspond to the primary storm tracks.

Unlike previous studies, no statistically significant trends in TCP volume, total rainfall, and TCP fraction were identified in the NAT between 1998 and 2011. Determining TCP trends requires long rainfall records. The TRMM record is still relatively short. Previous studies combined multiple datasets and so they might be affected by the bias of pre-SSM/I and post-SSM/I period (Lau and Zhou 2012). Also, the results are impacted by the selection of the TCP metric. However, TCP is highly correlated with TC frequency and intensity. Approximately 90% of the variance in TCP can be explained by the ACE index.

CHAPTER V

TCP AND TELECONNECTIONS

5.1 TCP and the North Atlantic Oscillation

5.1.1 NAO and Temporal Variations in TCP

The May to June (MJ) NAO index, June to November (JJASON) NAO index and winter (DJFM, December of the previous year to March) NAO index were calculated using the monthly NAO index. There is not an obvious relationship between TCP (green line) and the NAO indices (Figure 5.1). The scatter plot (Figure 5.2) and statistical test (Table 5.1) show a similar result. There is not statistically correlation between NAO and TCP in the NAT and its sub-basins. The May-June NAO and TCP over the Caribbean have a relatively strong negative correlation ($R^2 = 0.17$, $p= 0.07$). That is, when the May-June NAO increases, TCP decreases. On the contrary, a positive correlation have been identified between May-June NAO and TCP in the East Coast region.

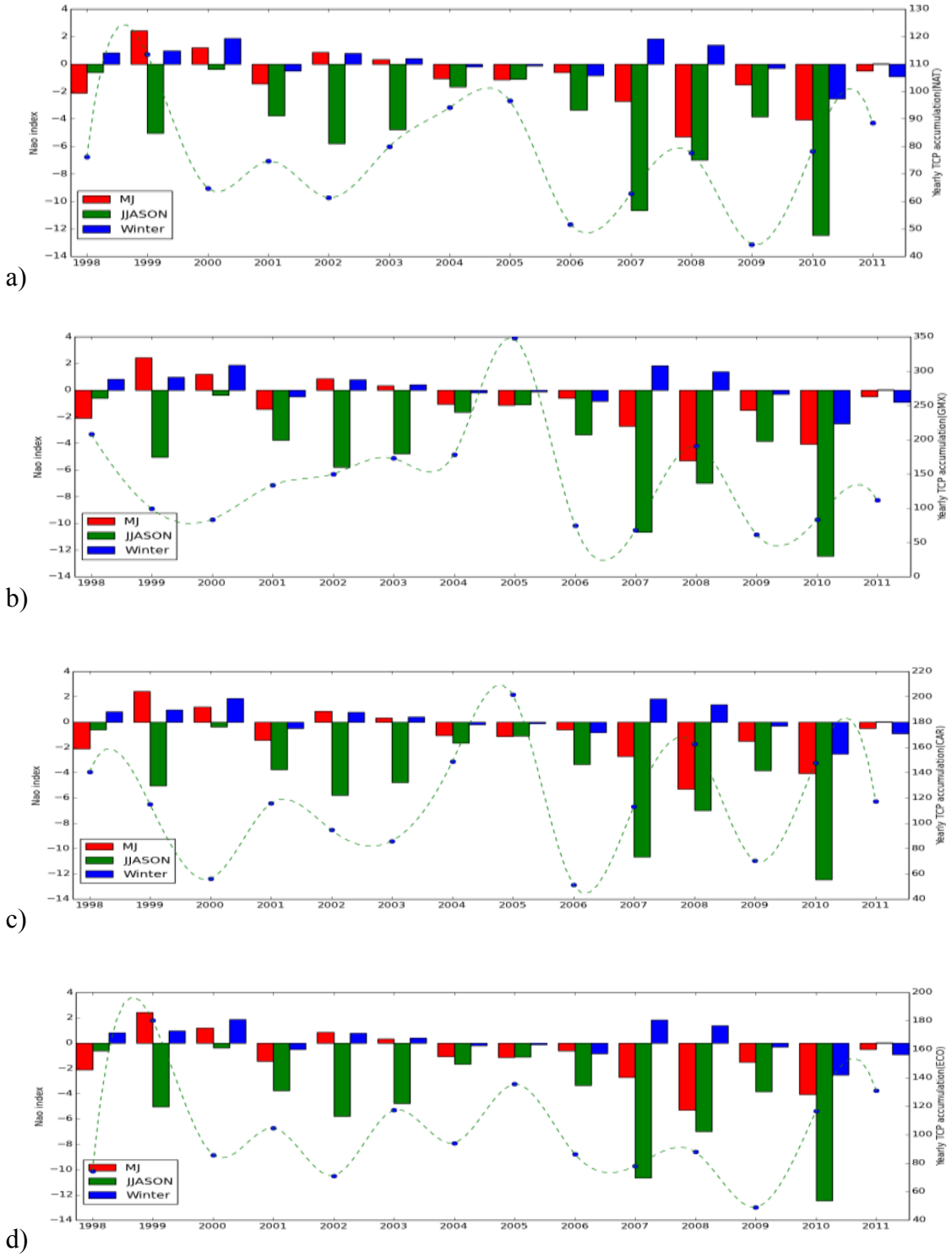

Figure 5.1. Time series of TC precipitation (mm) and NAO index (1998-2011) (a) NAT, (b) GMX, (c) CAR, and (d) ECO.

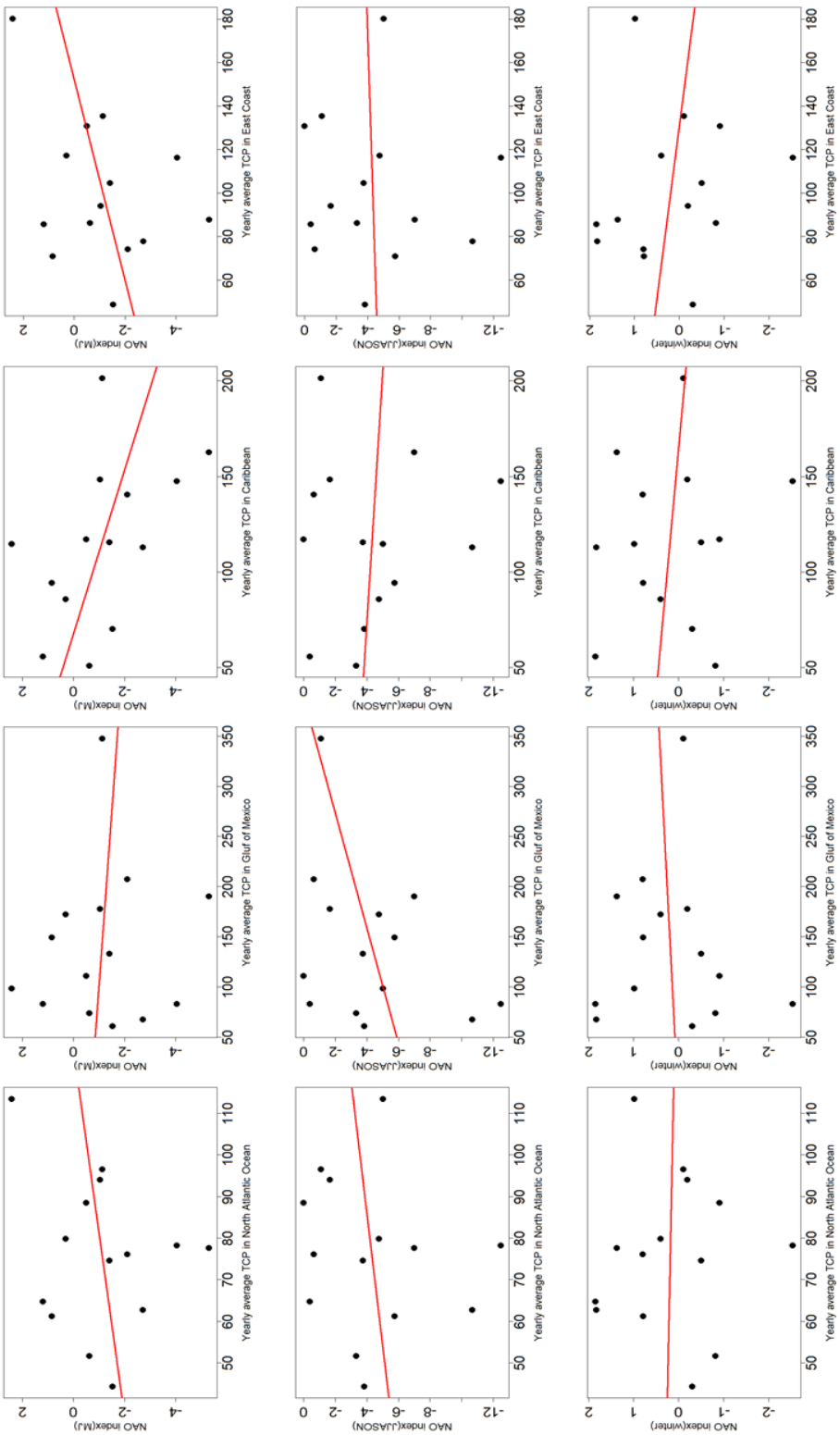

Figure 5.2. Linear regression model of NAO and TCP; rows: MJ, JJASON, winter (top to bottom); columns: NAT, GMX, CAR, ECO (left to right).

Table 5.1 Results of linear regression in terms of TCP and NAO

	NAT		*GMX*		*CAR*		*ECO*	
	R^2	P	R^2	P	R^2	P	R^2	P
MAY-JUN	0.04	0.48	0.01	0.71	0.17	0.07	0.12	0.21
JUL-NOV	0.02	0.60	0.12	0.20	<0.01	0.76	<0.01	0.89
DEC-MAR	0.05	0.44	<0.01	0.80	0.01	0.63	0.03	0.54

The result of the regression model analysis confirms the theory of straight moving hurricanes. The definition of the Straight-moving hurricanes is TCs that form in the tropics, go through from west to east, without recurvature, and ultimately make landfall in the CAR or along the GMX(Kossin et al. 2010). May-June NAO can influence the relative frequency of straight moving hurricanes because it reflects the strength of the North Atlantic subtropical high (Kossin et al. 2010). When early-summer NAO phase is negative, the subtropical high is weaker. This pattern can persist throughout hurricane season and it results in more straight moving hurricanes. This increases TCP in GMX and decreases TCP in CAR and ECO. On the contrary, when the May-June NAO is positive, it is associated with the opposite conditions.

Elsner and Jagger (2006) indicate that there is a negative relationship between the annual U.S. hurricane count and October-January NAO index (Figure 5.3(a)). We also find that there is a statistically significant positive correlation between TC count and annual mean TC precipitation in the North Atlantic for the period 1998-2011. However, the correlation between October-January NAO and TCP is not statistical significant. This may be result from the relatively short-term of records.

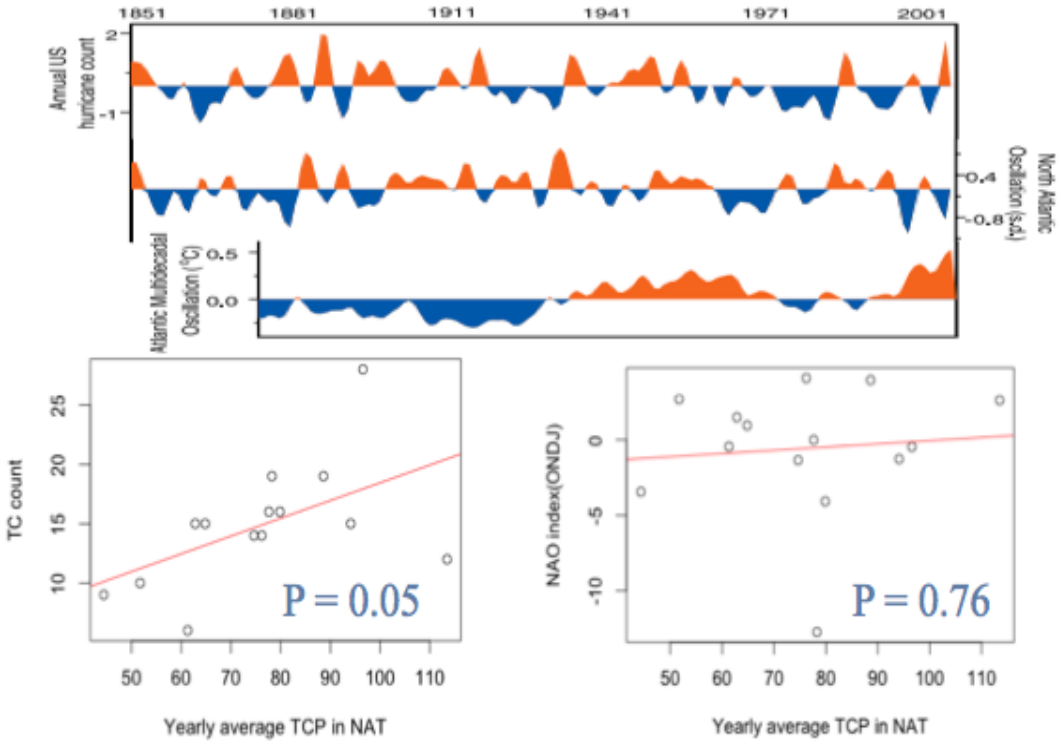

Figure 5.3 (a) Time series of annual U.S. hurricane counts and October–January North Atlantic Oscillation (Source: in Elsner and Jagger 2006), (b) Linear regression model of TC count and TC precipitation (mm) in NAT, and (c) Linear regression model of ONDJ NAO index and TC precipitation (mm) in NAT.

5.1.2 NAO and Spatial Variations in TCP

The May-June NAO index was used to determine positive and negative NAO years. For the time period of 1998 to 2011, the following years are positive NAO years: 99/00, 00/01, 02/03, and 03/04. Correspondingly, the following years are negative NAO years: 98/99, 01/02, 04/05, 05/06, 06/07, 07/08, 08/09, 09/10, 10/11 and 11/12. Mean TCP in the positive (Figure 5.4a) and the negative May-June NAO years (Figure 5.4b) was calculated. Compared with the negative NAO years, the locations with highest values of TCP in the positive NAO years are more dispersed. The regions with greatest TCP are primarily located along the East Coast of the U.S. and in the middle of North Atlantic Ocean along 20°N.

However, in negative NAO years, TCP mainly occurs in the Caribbean and the Gulf of Mexico. Figure 5.4c shows the difference in TCP between the positive and negative NAO years (positive years – negative years). The blue colors in Figure 5.4c show regions where TCP in negative years is greater than in positive years and the red colors show the opposite. The Caribbean has higher mean TCP in negative NAO years. On the contrary, the East Coast region and the area around Bermuda have higher TCP in positive NAO years. These results corresponded to the “straight moving” hurricane theory.

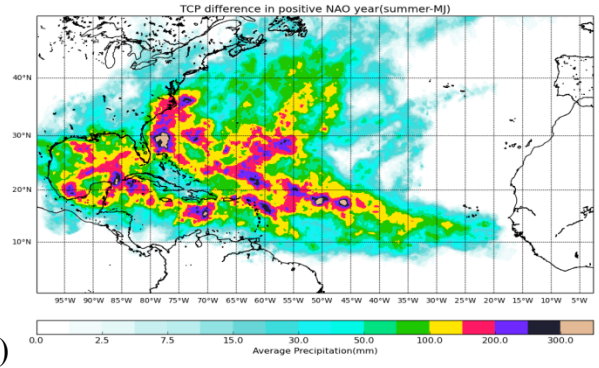

(a)

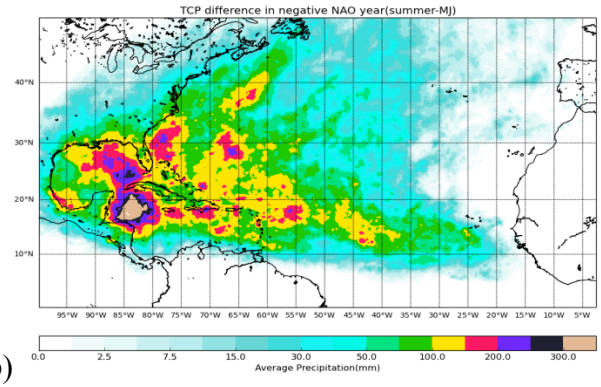

(b)

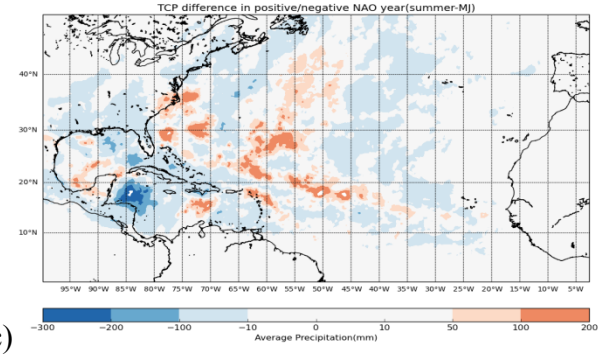

(c)

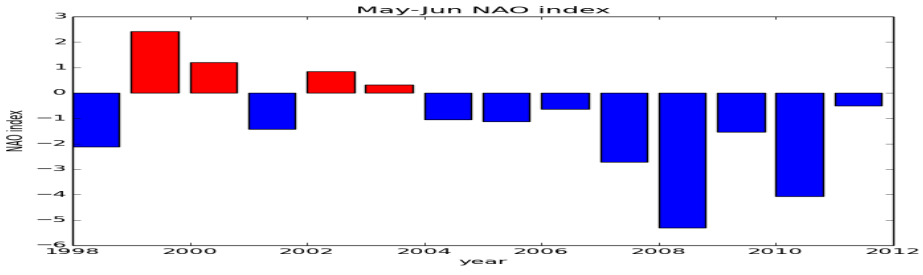

(d)

Figure 5.4. TCP (mm) with respect to the phase of the NAO: (a) positive NAO years, (b) negative NAO years (c), difference between positive and negative NAO years, and (d) mean May-June NAO (1998-2012).

Pearson correlations between TCP and the May-June NAO index were calculated for each grid cell (Figure 5.5). Only the statistically significant correlations ($P < 0.05$) are shown in the plot. Similar to the distribution of differences between positive and negative May to June NAO years, the correlations are positive in the East Coastal region, and negative in the Caribbean islands and the central part of United States. In terms of the Atlantic Ocean, there are some negative correlations with NAO in the eastern Atlantic and some negative spots in the western Atlantic. This spatial pattern again confirms the theory that the positive NAO will enhance the sub-tropical high and will tend to block straight-moving TCs. As shown in Figure 5.5, there are some statistically significant correlationa in the Caribbean islands, central U.S., and the Great Lakes region. It seems that the influence of NAO on TCP is greater over land. In the spatial correlation between TCP and JASON NAO index, there are some positive correlations in the northern Atlantic and negative correlations in eastern Atlantic, southwestern of U.S., and in the middle of the Caribbean. For the winter, almost all of the significant correlations are negative and most of them located in eastern of North Atlantic.

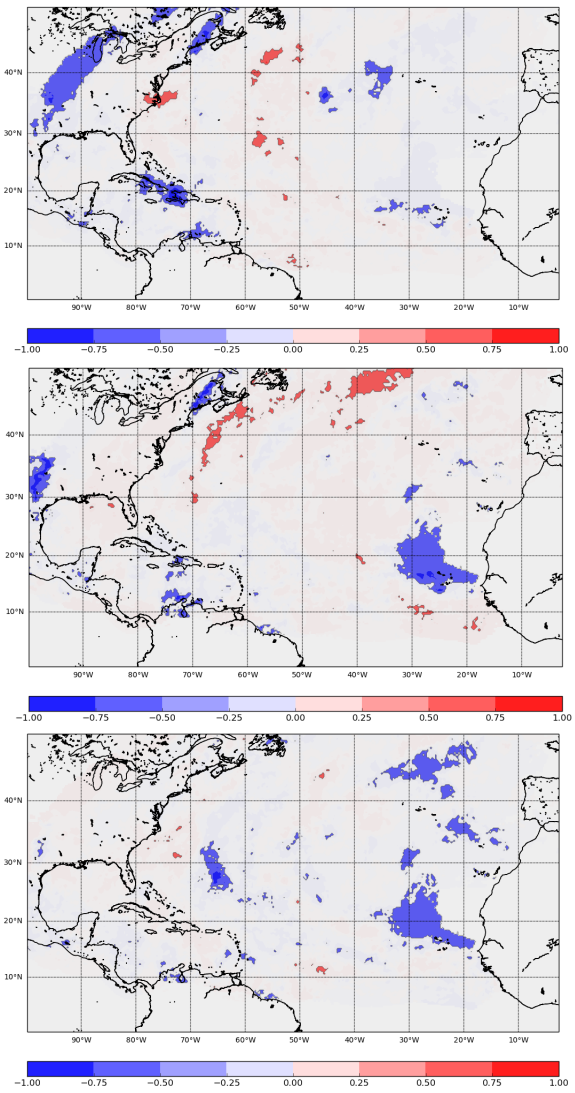

Figure 5.5. Correlation between TCP and NAO in the Atlantic: (a) MJ (upper left), (b) JJSON (upper right), and (c)Winter (lower right)

5.2 TCP and ENSO

5.2.1 ENSO and Temporal Variations in TCP

The El Niño/Southern Oscillation (ENSO) is significant to inter-annual climate variability. Past studies have shown that ENSO can impact seasonal TC activity (Gray 1984a; Patricola et al. 2014). During a La Niña, there tends to be more TCs in the Atlantic than usual, while during an El Niño there tend to be fewer. El Niño events are related to a weakening of the Walker circulation, which leads to an increase of westerly winds in upper troposphere over the tropical Atlantic. The enhanced wind shear tends to inhibit the genesis of TC. On the contrary, in La Niña years the environment is more suitable for TCs to develop.

There are many ENSO indices, for example: Nino 3.4 SST, SOI and MSLP, used in related studies. This study uses the multivariate ENSO index (MEI; Wolter, 1987) (www.cdc.noaa.gov/people/klaus.wolter/MEI/table.htm). The MEI contains more information than some other indices. It can be thought as a weighted mean of the major ENSO features and it includes the following variables: sea-level pressure, surface wind, sea surface temperature, surface air temperature, and cloudiness (Wolter and Timlin 1993, 1998). MEI index was calculated for 4 different time periods: DJF MEI, MAM MEI, JJA MEI and SON MEI.

ENSO is not strongly correlated with TCP (Figure 5.6 and Figure 5.7). Generally, TCP has a negative correlation over the entire North Atlantic. The September to November MEI has the highest correlation ($R^2 = 0.22$) with TCP in the North Atlantic

(Table 5.2). TCP tends to decrease during El Niño events. These results are in accord with past researches(Zhu et al. 2013; Rodgers et al. 2001; Jiang and Zipser 2010).

The results are more variable in the sub-basins. TCP in the CAR and ECO has a relatively high negative correlation with the September to November MEI. The ECO is negatively associated with the MEI within the pre-hurricane season (March to May). The DJF MEI indices show weak correlations with TCP in the whole region and all sub-basins.

Table 5.2 Results of linear regression in terms of TCP and MEI

	NAT		*GMX*		*CAR*		*ECO*	
	R^2	P	R^2	P	R^2	P	R^2	P
DJF	<0.01	0.96	0.13	0.21	0.11	0.25	0.02	0.60
MAM	0.04	0.48	0.17	0.14	0.05	0.45	0.21	0.10
JJA	0.15	0.17	0.05	0.46	0.10	0.27	0.20	0.11
SON	0.22	0.10	≈0	0.99	0.21	0.10	0.20	0.10

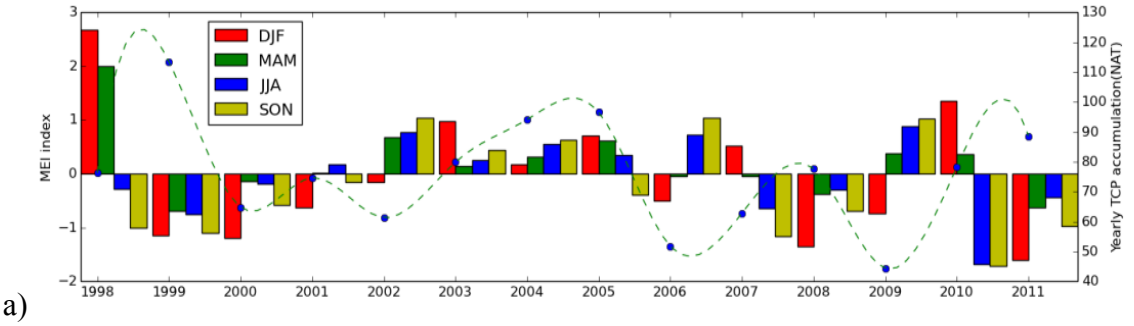

a)

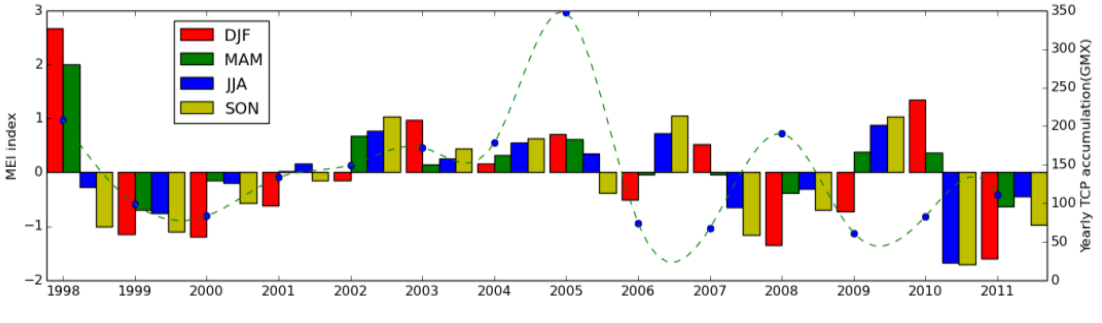

b)

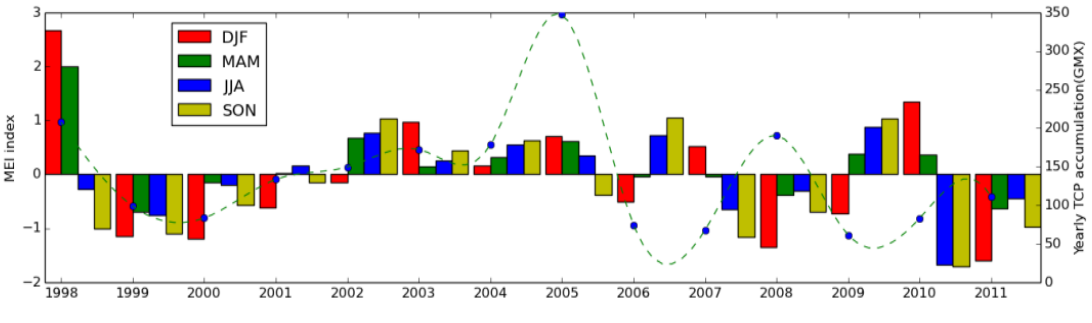

c)

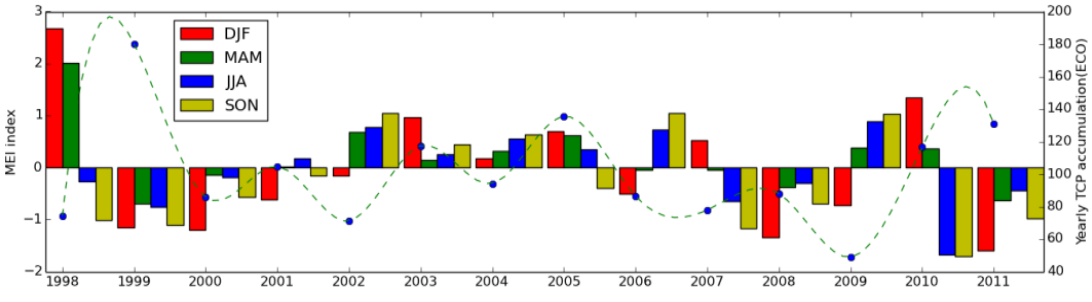

d)

Figure 5.6. Time series of TCP (mm) and MEI (1998-2011) (a) NAT, (b) GMX, (c) CAR, and (d) ECO.

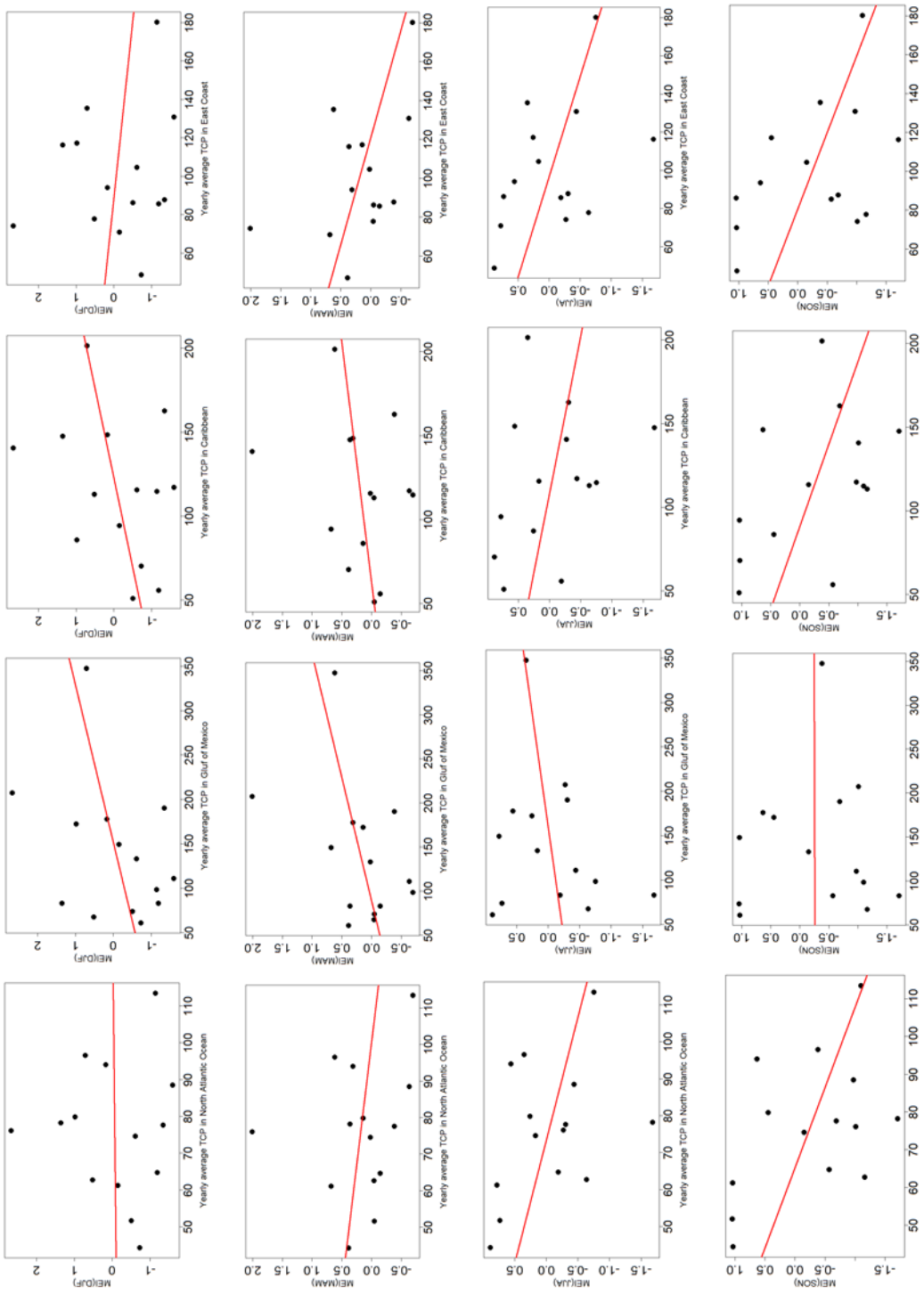

Figure 5.7. Linear regression models of MEI and TCP; rows: DJF, MAM, JJA, and SON (top to bottom); columns: NAT, GMX, CAR, ECO (left to right).

5.2.2 ENSO and Spatial Variations in TCP

El Niño years and La Niña years were identified using the MEI. The MEI within the period between Dec 1949/Jan 1950 and May/Jun 2014 was ranked from lowest (strongest La Niña event) to highest (strongest El Niño event). El Niño and La Niña years were selected based on rank of at least 5 consecutive months MEI index (Kuleshove et al. 2008; Trenberth 1997). Therefore, for the time period of 1998 to 2011, the following years are identified as El Niño seasons: 2002/03, 2004/05, 2006/07 and 2009/10. Correspondingly, the following years are considered as La Niña seasons: 1998/99, 1999/00, 2007/08, 2010/11 and 2011/12.

Figure 5.8a and 5.8b shows that there is much more TCP during La Niña years than El Niño years, especially in east coast of United States and the central Atlantic Ocean. The one exception is a region of high TCP in eastern part of the Gulf of Mexico. This value may result from very high precipitation in some specific years.

Based on the results shown in Figure 5.8c, there are much more TCP in El Niño years than La Niña years in GMX, southeastern of U.S. and North Caribbean Sea. There is greater TC rainfall in La Niña years in the majority of the NAT.

These results are generally consistent with past research (Jiang and Zipser 2010; Rodgers et al. 2001). In Atlantic Ocean, generally, a decrease in TC rainfall was found under El Niño years. However, Rodgers et al. (2001) does not show an obvious increase in TCP in the eastern GMX in El Niño years. Jiang and Zipser (2010) shows a similar spatial pattern, however the differences between El Niño and La Niña are much smaller in their study.

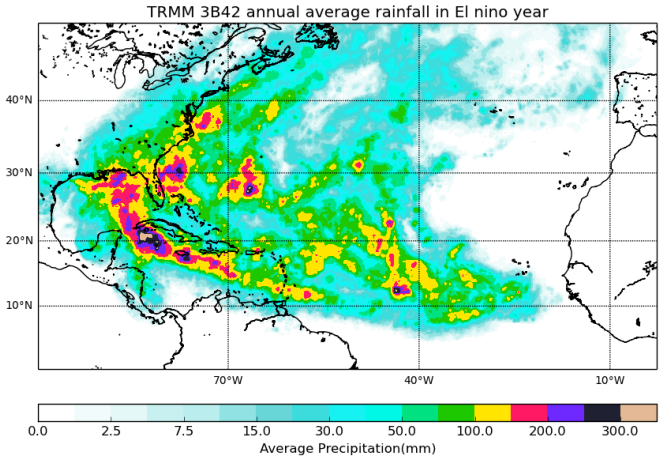

(a)

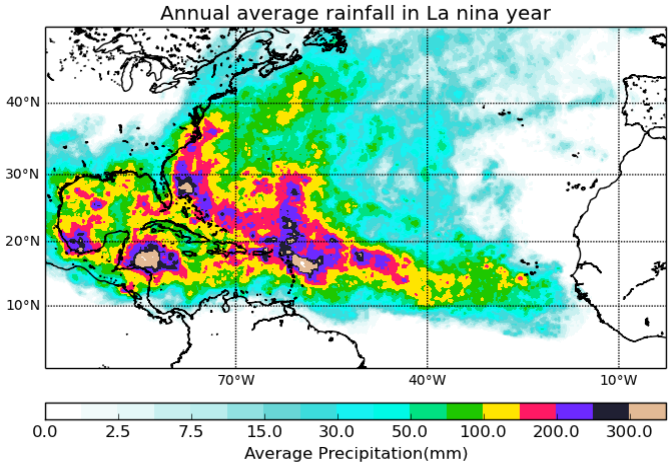

(b)

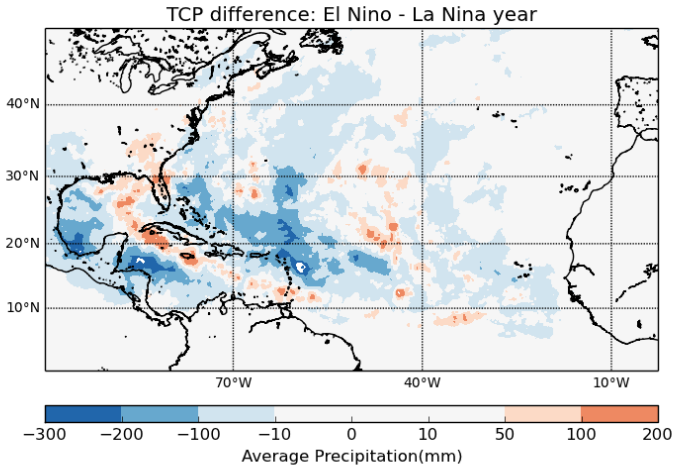

(c)

Figure 5.8. TCP (mm) with respect to the phase of the ENSO (a) El Niño years, (b) La Niña years, and (c) difference between El Niño and La Niña years

Correlation analysis was also applied. Statistically significant correlations between TCP and 3-month MEI are shown in Figure 5.9. The pattern of the correlation varies with the seasons. The correlation distribution has an opposite pattern in winter/spring and summer/fall. The westerly winds in upper troposphere over Caribean basin as well as the equatorial Atlantic will increase when an El Niño event occurrs (Gray, 1984a). Increased westerly wind will enhance vertical wind shear and finally lead to decrease of TC activity as well as TCP. This is the reason why there is negative correlation shown in most of the North Atlantic (Figure 5.9c, d). In JJA and SON, the majority of the North Atlantic shows negative correlations between TCP, especially in the Caribbean and the coastal region in the western GMX. Generally, the correlations are relatively weak in most of the North Alantic. In the contrast, the spatial correlations in DJF and MAM have the opposite pattern. Postive correlations were identified in eastern Atlantic Ocean, central North America, Gulf of Mexico and the Caribean basin. The correlation coefficient in DJF and MAM are even stronger than JJA and SON. As shown in Figure 5.10, years with a positive MEI in DJF and MAM always have a negative MEI in JJA and SON, and vice versa. In addition, the variablity of the MEI in DJF and MAM is higher than in JJA and SON. This may explain the seasonal variations in the spatial correlations between the MEI and TCP.

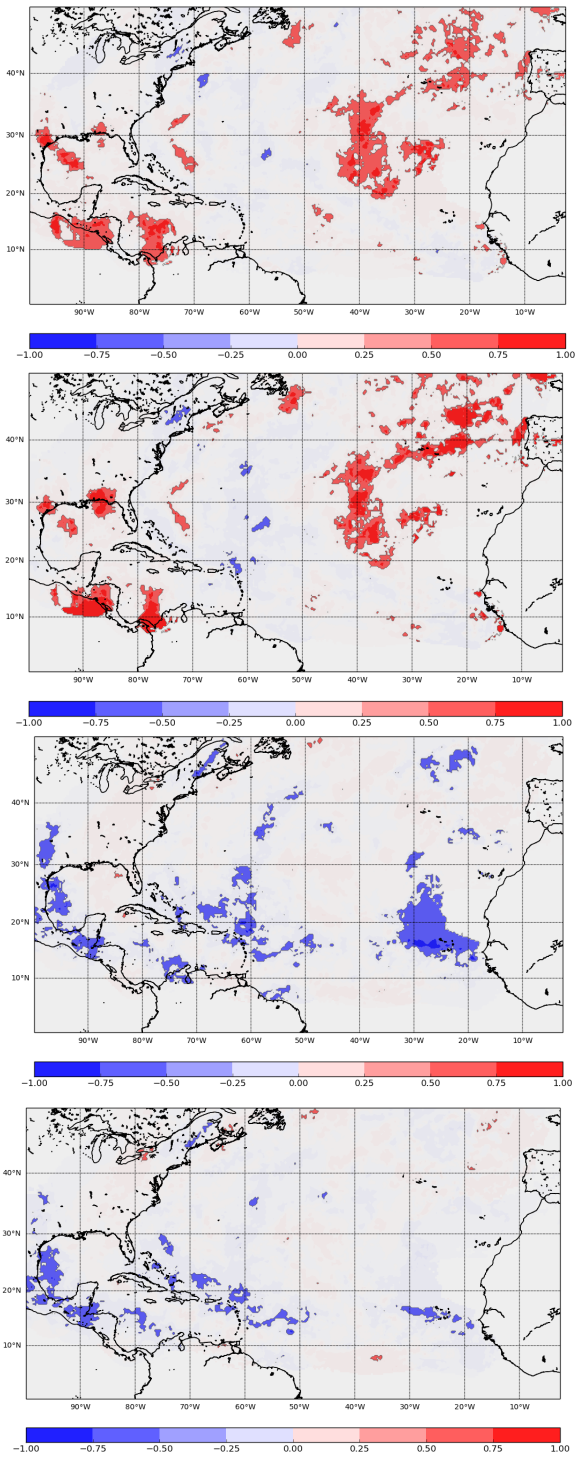

Figure 5.9. Correlation between TCP and ENSO in the Atlantic: (a) DJF (upper left), (b) MAM (upper right), (c) JJA (lower left), and (d) SON (lower right).

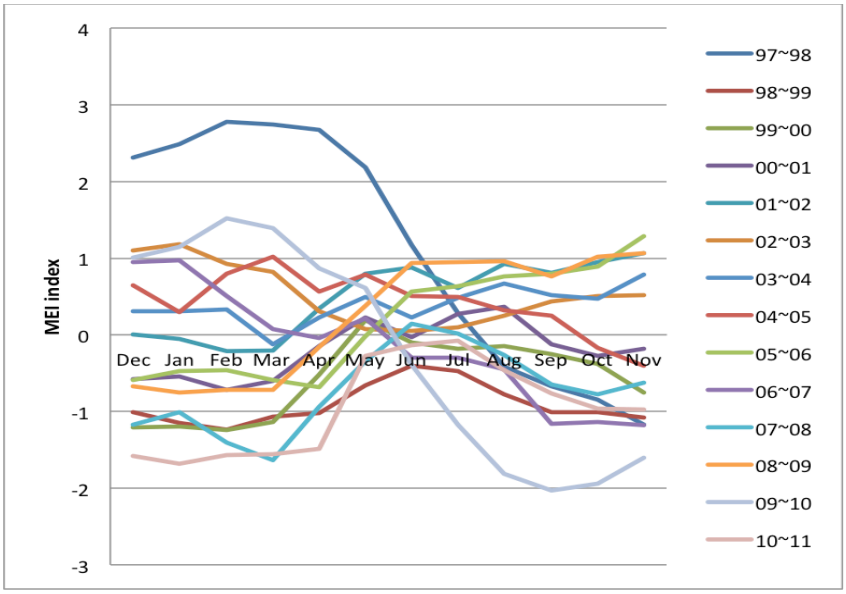

Figure 5.10. Monthly evolution of MEI (1997-2011).

5.3 TCP and Quasi Biennial Oscillation

5.3.1 QBO and Temporal Variation in TCP

The index of QBO is a measure of both strength and direction of the equatorial zonal wind. The mean QBO index was calculated for each season: DJF, MAM, JJA, and SON. Positive QBO index corresponds to westerly wind while negative values to easterly wind.

Variations of TCP in each sub-basin and QBO are shown in Figure 5.11 and Figure 5.12. There is an extremely weak correlation ($R^2 < 0.1$) between seasonal QBO and TCP in North Atlantic and every sub-basin (Table 5.3). None of the models are statistically significant. This result agrees with previous research (Camargo and Sobel 2010) that found that the relationship between TC activity and QBO became very weak after the 1980s.

Table 5.3 Results of linear regression in terms of TCP and QBO

	NAT		*GMX*		*CAR*		*ECO*	
	R^2	P	R^2	P	R^2	P	R^2	P
DJF	<0.01	0.93	0.01	0.73	0.08	0.33	0.01	0.70
MAM	0.01	0.71	0.03	0.56	0.03	0.53	<0.01	0.82
JJA	0.02	0.65	0.08	0.34	0.04	0.84	0.02	0.60
SON	0.01	0.72	0.12	0.22	0.01	0.70	<0.01	0.78

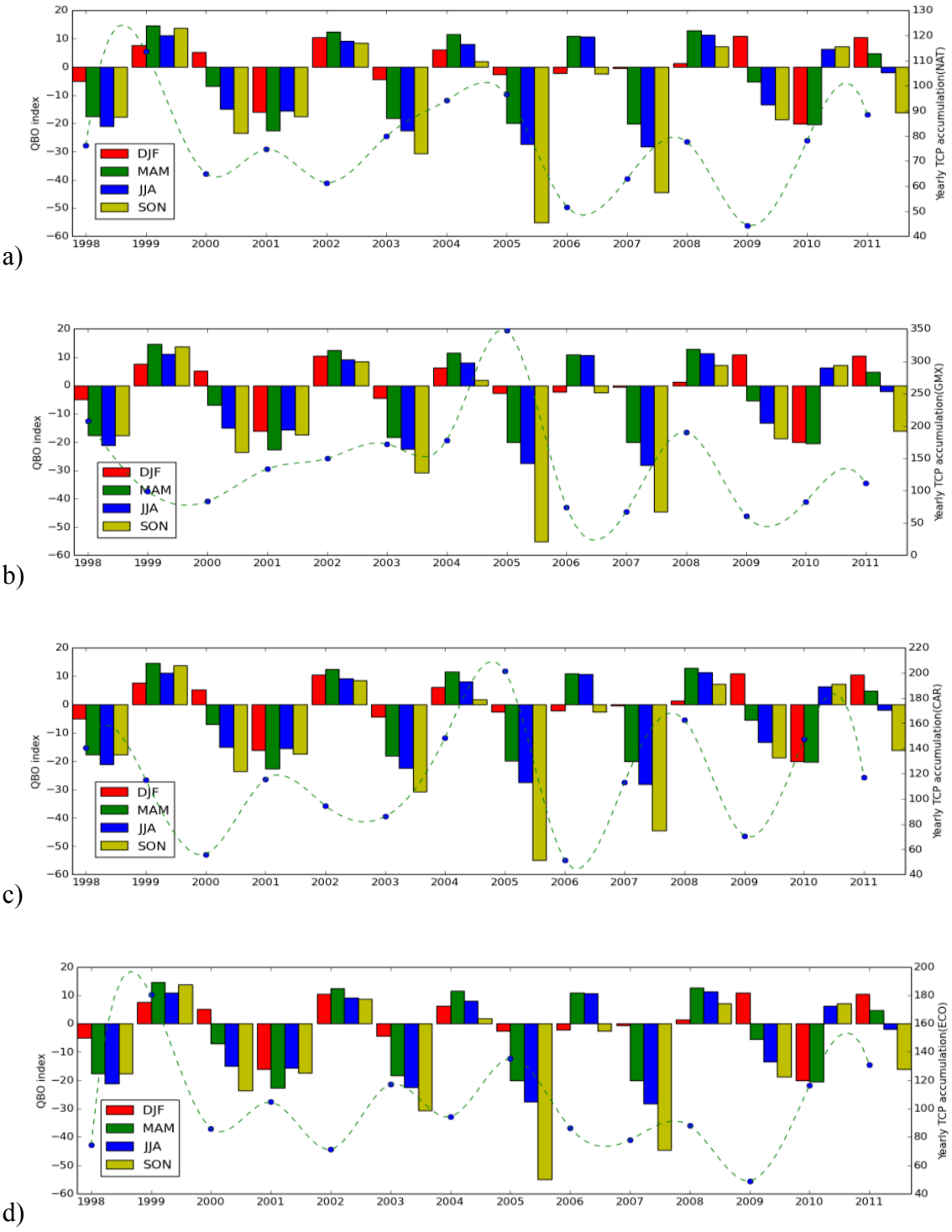

Figure 5.11. Time series of TCP (mm) and QBO (1998-2011) (a) NAT, (b) GMX, (c) CAR, and (d) ECO.

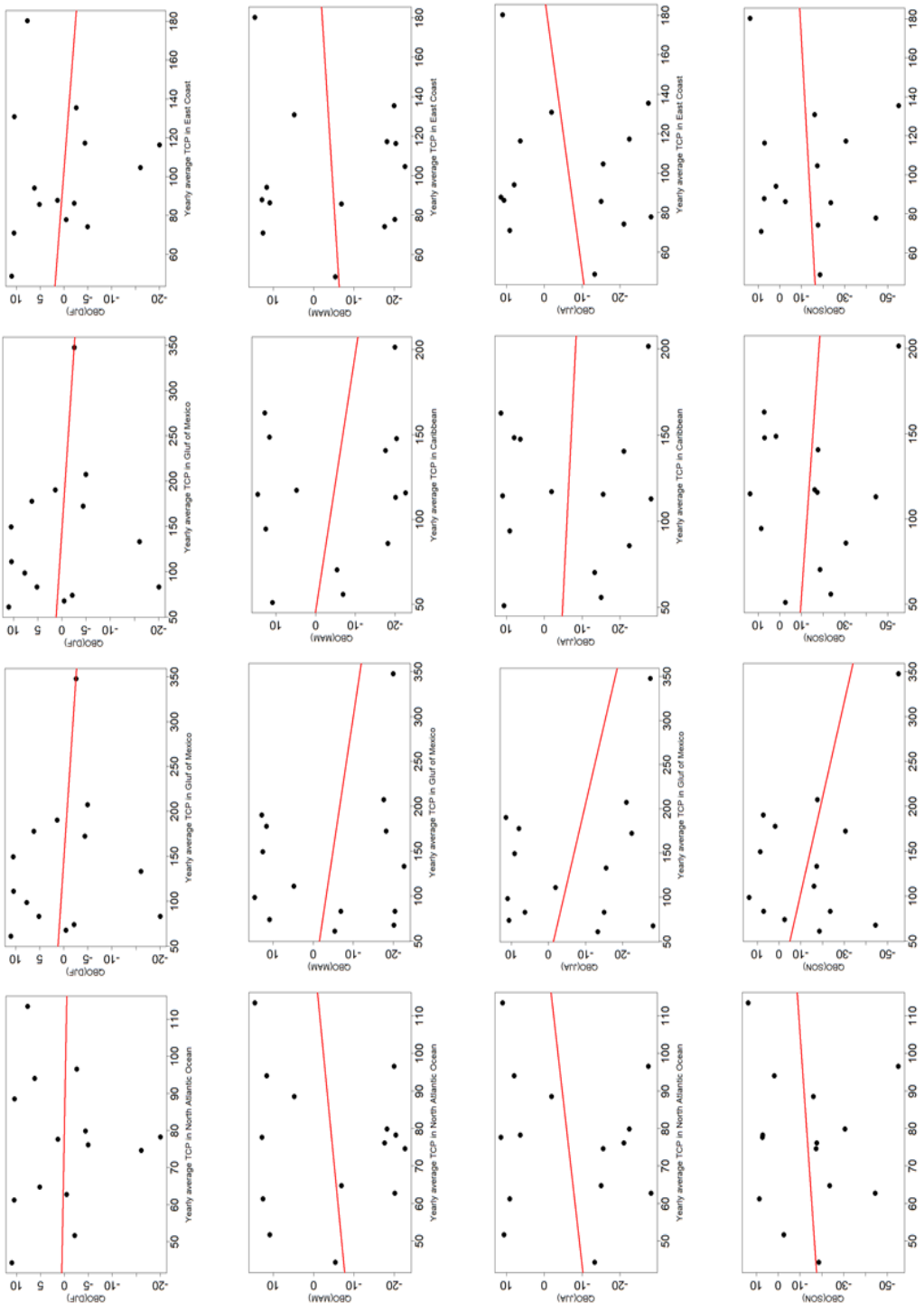

Figure 5.12. Linear regression models of QBO and TCP; rows: DJF, MAM, JJA, and SON (top to bottom); columns: NAT, GMX, CAR, ECO (left to right).

5.3.2 QBO and Spatial Variations in TCP

Similar with the analysis before, the distribution of TCP in QBO positive year and negative year was identified. The monthly 30 mb QBO index was used to calculate the annual mean QBO. Years with positive values were identified as a positive QBO year, while years with negative values were identified as a negative QBO year. Therefore, the positive (westerly) QBO years are following years: 1998/99, 2000/01, 2001/02, 2003/04, 2005/06, 2007/08, 2009/10, and 2010/11. Correspondingly, the following years are considered as negative (easterly) QBO seasons: 1999/00, 2002/03, 2004/05, 2006/07, 2008/09, and 2011/12. The distributions of TCP in positive and negative QBO year in the North Atlantic are shown in Figure 5.13. ENSO years were not excluded, as Gray (1984a) did, given the short period of record. The relationship between ENSO and QBO is still uncertain. In the early record, the correlation between QBO and ENSO is negative, that is El Niño events are more common in the easterly QBO years while La Niña events are more common when QBO is westerly. However, in the later part of the record, the situation is opposite.

In terms of spatial patterns, TCP in positive QBO years is stronger in a relatively large region, while in the negative QBO years the TCP is more centralized and weaker (Figure 5.13). In positive QBO years (Figure 5.13a), the majority of the highest TCP is found along the coastal areas of Florida as well as in the Caribbean. While Figure 5.13b shows that during negative QBO years, maximum precipitation occurred over northwest CAR. Figure 5.13c reveals that TCP is greater during positive QBO years over northeastern part of CAR as well as eastern coast of U.S. However, during negative

QBO years, TCP is greater over the western part of CAR, southern part of continent of North America, Gulf of Mexico, and some regions in mid-latitude of western NAT. Generally, the differences between the positive and negative QBO years are not as obvious when compared with other teleconnections such as ENSO or NAO.

The seasonal variability in the correlations between QBO and TCP of the spatial correlation pattern is small (Figure 5.14). Based on past research (Gray 1984a, Camargo and Sobel 2010), when 30 hPa stratospheric winds are from the west, hurricanes are more frequent. Therefore, there should be strong positive correlations in the study region. However, we do not see this pattern in the correlations of QBO and TCP in the North Atlantic, at least, not in the period from 1998 to 2011. There are more statistically significant negative correlations in the research region, specifically in the southern NAT as well as the Caribbean. Also, some statistically significant positive correlations are located along the ECO of U.S., especially for the MAM QBO index.

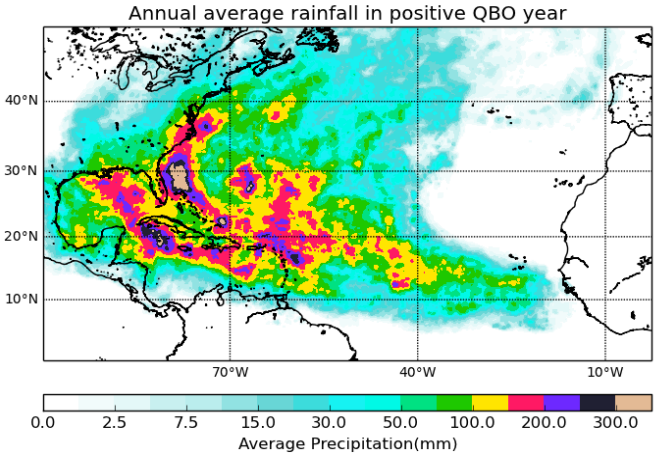

a)

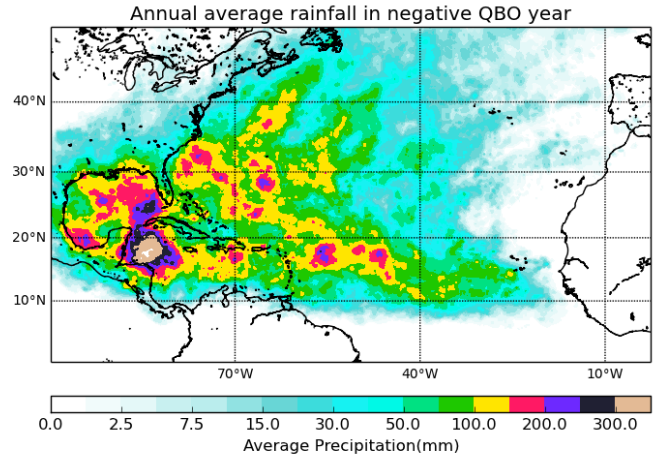

b)

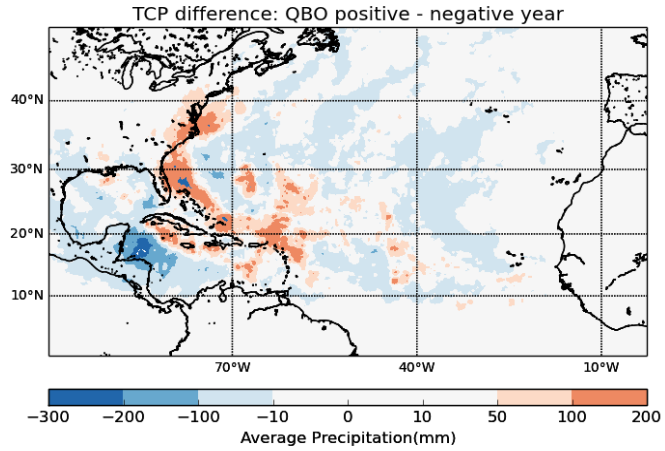

c)

Figure 5.13. TCP (mm) with respect to the phase of the QBO (a) QBO positive years, (b) QBO negative years, and (c) difference between positive QBO years and negative QBO years.

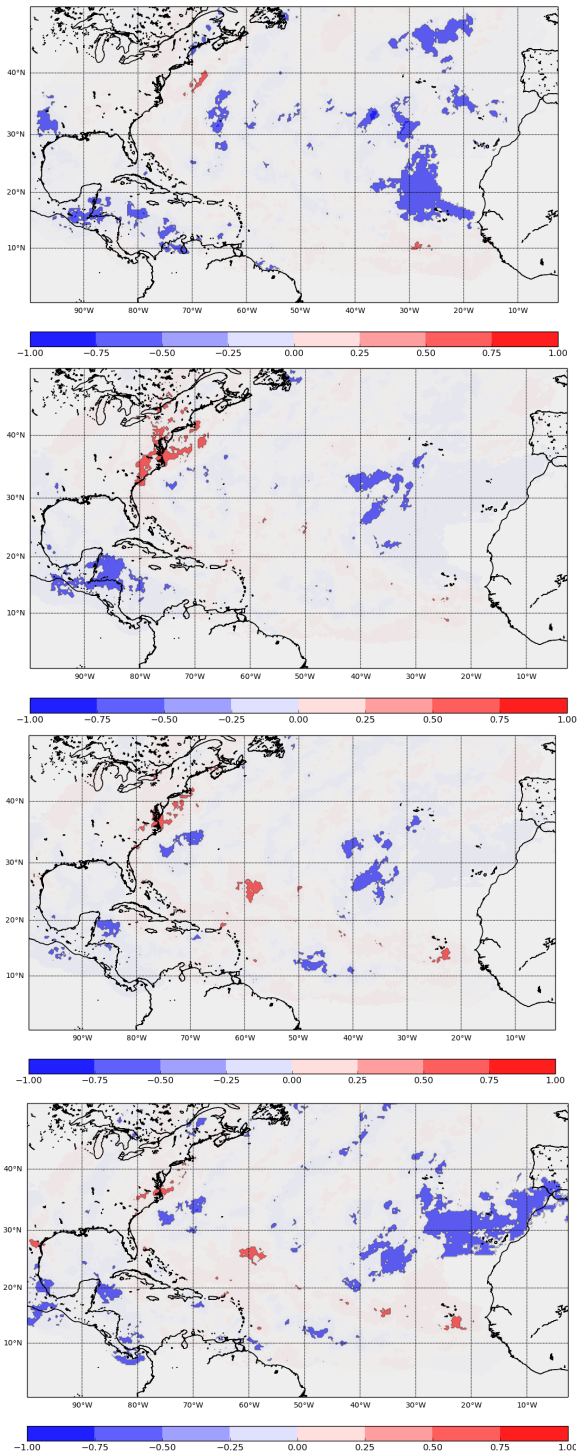

Figure 5.14. Correlations between TCP and QBO: (a) DJF (upper left), (b) MAM (upper right), (c) JJA (lower left), and (d) SON (lower right).

5.4 TCP and Atlantic Meridional Mode

5.4.1 AMM and Temporal Variation in TCP

The monthly AMM index was divided into 4 seasonal groups: DJF, MAM, JJA, and SON. Figure 5.15 shows the variations of AMM in each season and in different sub-basins. Correlations between AMM and TCP were calculated for each basin and the scatter plots and statistical results are shown below (Figure 5.16 and Table 5.4). Correlations between AMM and TCP are stronger during the hurricane season, especially from June to August. Compared with other basins, TCP in CAR has stronger correlations during the whole year. In addition, compared with other teleconnections the AMM index shows highest correlation ($R^2 = 0.45$) with TCP in CAR in JJA. That is, in terms of temporal variation, AMM exerts a greater impact on TCP in the Caribbean region in both pre-hurricane season (MAM) and hurricane season (JJA).

Based on previous research (Vimont and Kossin, 2007), the AMM is positively associated with SST, low-level vorticity, and convergence and it is negatively associated with sea level pressure and vertical wind shear. Therefore, AMM is an indicator of Atlantic climatic conditions that are closely related with seasonal TC activity, as well as TCP. This is one reason why TCP is strongly connected with AMM. During the hurricane season, the climatic conditions will influence the track and intensity of TCs. However, the reason of the difference between sub-basins is still uncertain.

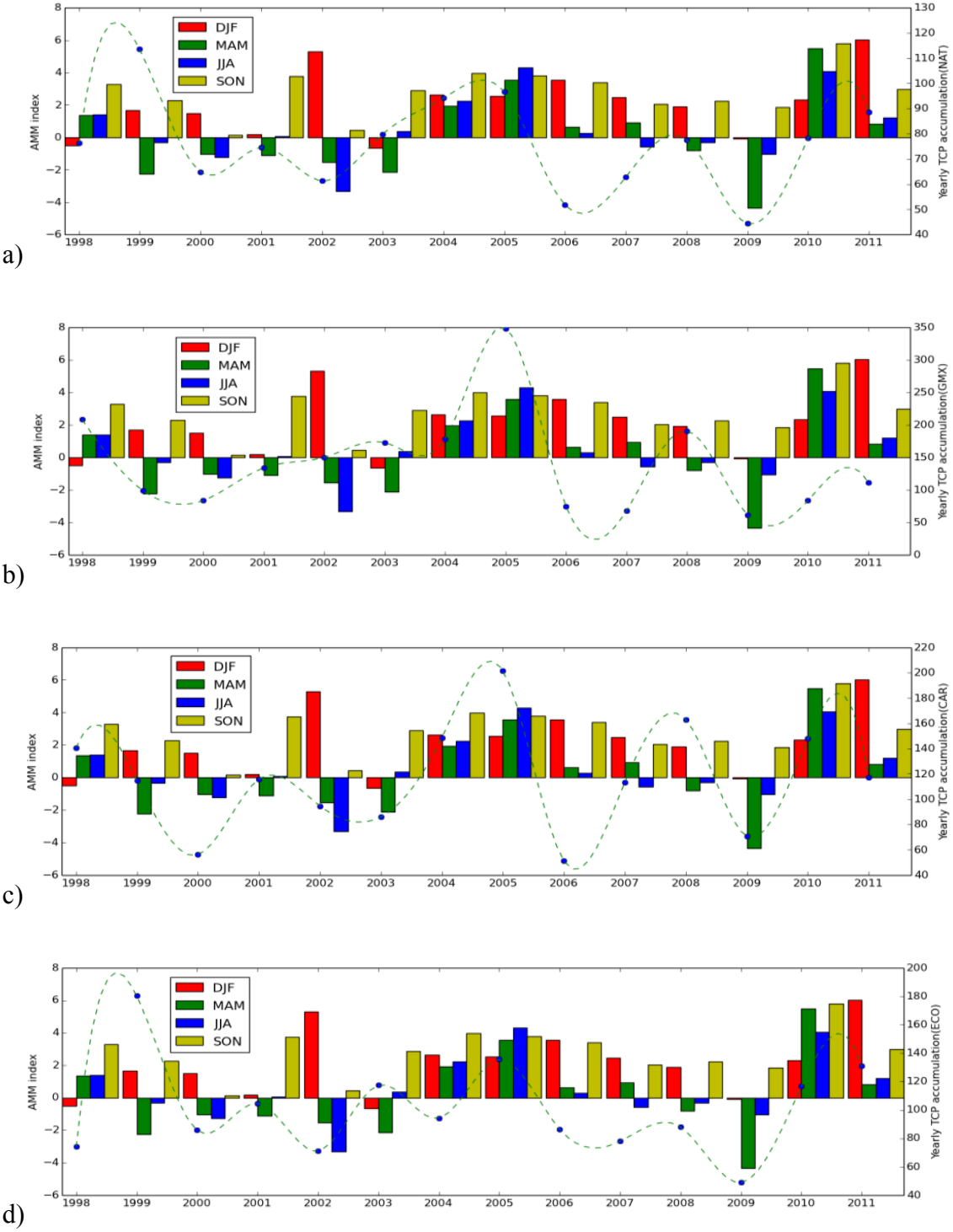

Figure 5.15. Time series of TCP (mm) and AMM (1998-2011) (a) NAT, (b) GMX, (c) CAR, and (d) ECO.

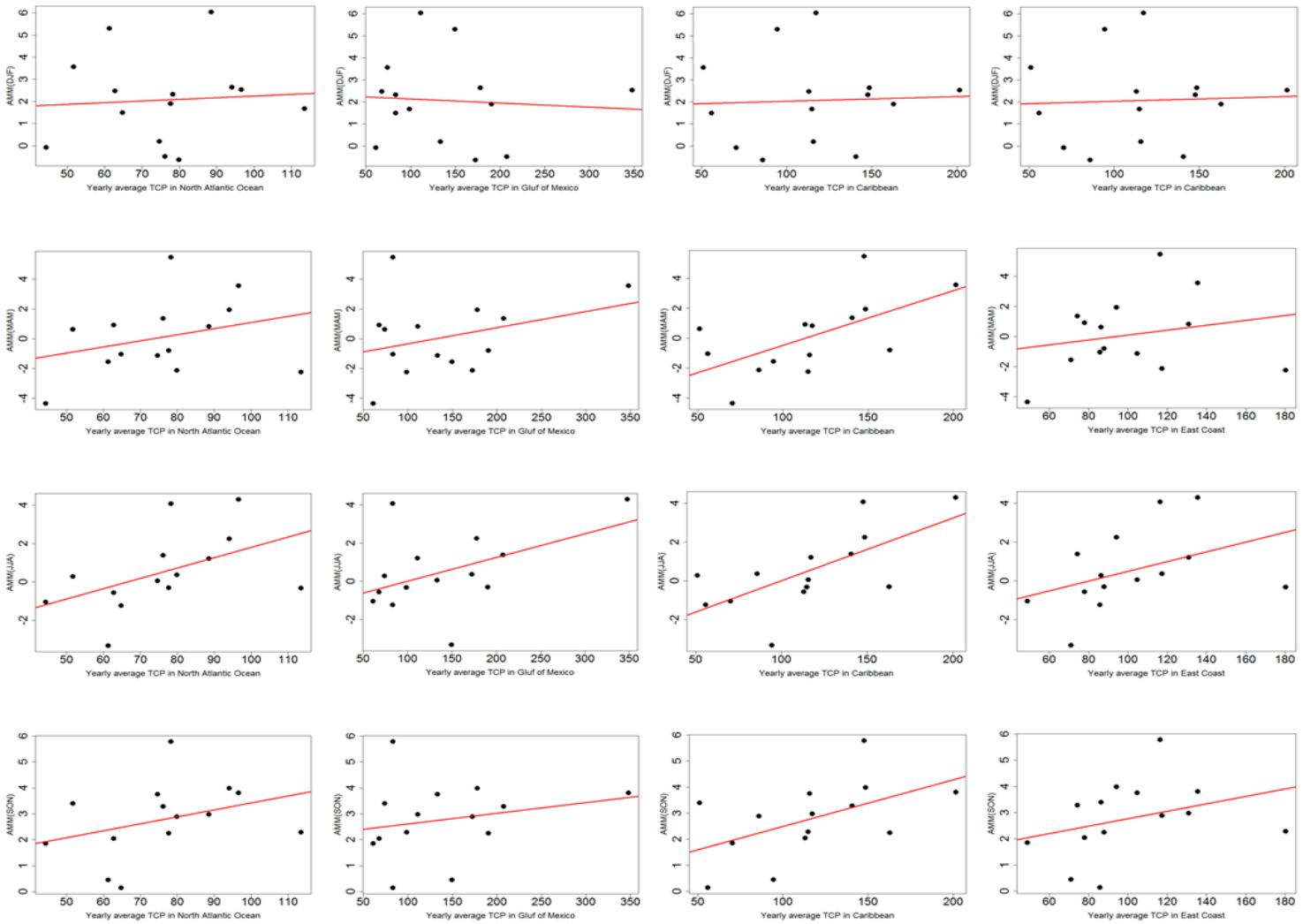

Figure 5. 5.16. Linear regression models of AMM index and TC rainfall; rows: DJF, MAM, JJA, and SON (top to bottom); columns: NAT, GMX, CAR, ECO (left to right).

Table 5.4 Results of linear regression in terms of TCP and AMM

	NAT		*GMX*		*CAR*		*ECO*	
	R^2	P	R^2	P	R^2	P	R^2	P
DJF	<0.01	0.82	0.01	0.80	0.08	0.88	0.02	0.65
MAM	0.09	0.30	0.11	0.25	**0.37**	**0.02**	0.05	0.46
JJA	0.24	0.08	0.22	0.09	**0.45**	**<0.01**	0.17	0.15
SON	0.12	0.23	0.05	0.45	0.26	0.06	0.11	0.26

5.4.2 AMM and Spatial Variations in TCP

Monthly AMM values were used to calculate the mean annual AMM. Years with a positive AMM value are identified as a positive AMM year, and vice versa. The negative AMM years are: 2000/01, 2002/03, and 2009/10. All other years over the period 1998 to 2011 are identified as positive AMM years. The mean annual TCP in those years in each grid cells was calculated. The distributions of TCP in AMM positive years and AMM negative years are displayed in Figure 5.17a, b.

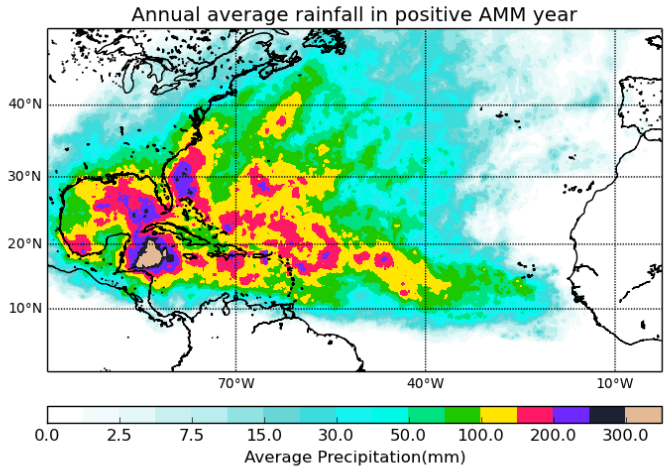

a)

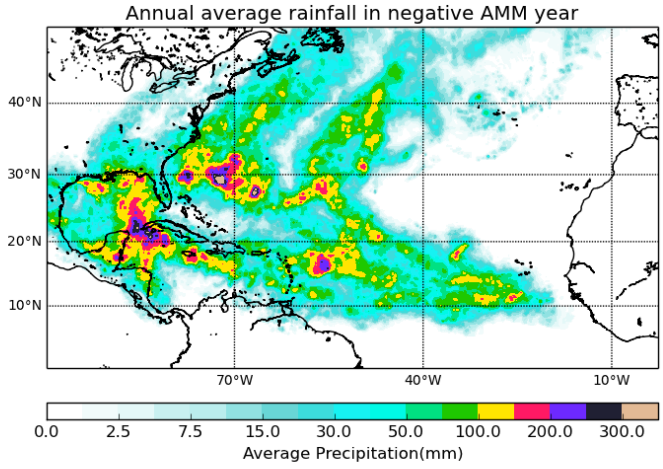

b)

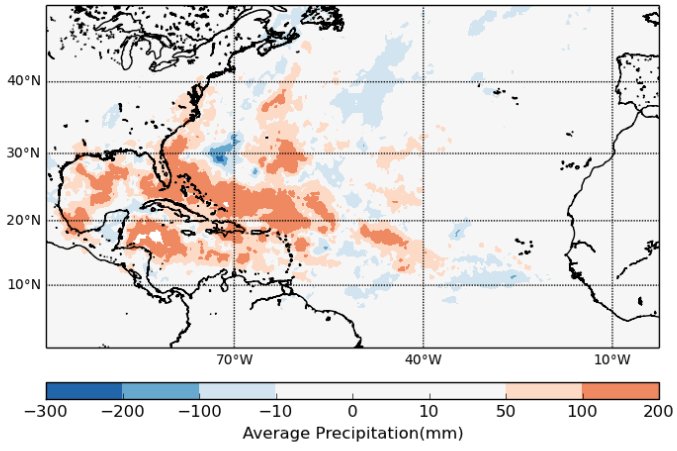

c)

Figure 5.17. TCP (mm) with respect to the phase of the AMM: (a) AMM positive years, (b) AMM negative years, and (c) difference between positive AMM years and negative AMM years.

Generally, in positive AMM years TCP is much greater than in negative AMM years. There is a positive relationship between AMM and TCP in NAT and its sub-basins. The highest TCP in positive AMM years is located in the northern CAR. In the negative AMM years, the region with the greatest TCP is in the northern GMX. Almost all of the differences between positive and negative AMM years are greater than zero. Therefore, TCP is greater during positive AMM years. The only exception is a small region over eastern NAT.

Spatial correlation analysis was applied to identify the correlation between TCP and AMM. The result shows that besides DJF, the patterns of the correlation between TCP and three other AMM index are similar (Figure 5.18.). In DJF, the correlations between TCP and AMM index are weak. We only find statistically significant correlations in a few small regions (Figure 5.18(a)). Specifically, positive correlations in southeastern NAT and northern NAT near east coast of U.S., and negative correlations in the middle of NAT. However, in MAM, JJA, and SON, the correlations in NAT are almost all positive, especially in Central American, Caribbean and eastern of NAT. These results agree with the previous results. Based on the spatial correlation analysis, the correlation in Caribbean is stronger than other sub-basin in the region. Therefore, during the hurricane season, the AMM has a positive correlation with TCP in the NAT basin. TCP in Caribbean also has a statistically significant positive correlation with AMM index.

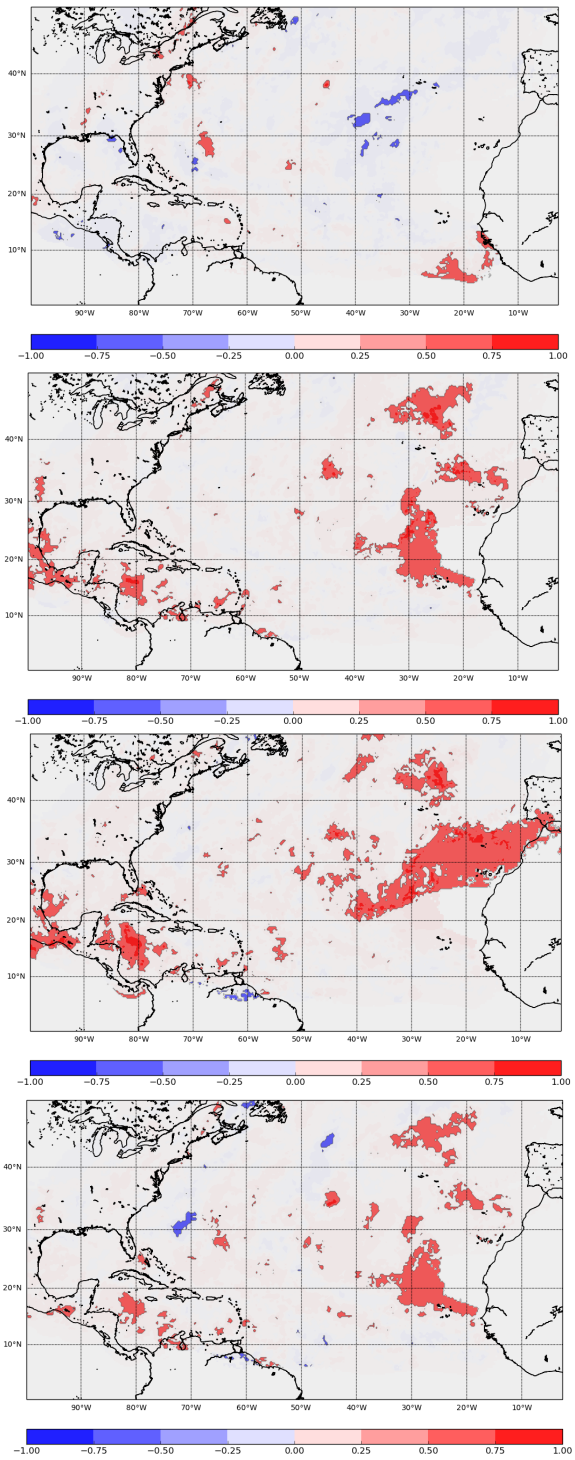

Figure 5.18. Correlations between TCP and AMM: (a) DJF (upper left), (b) MAM (upper right), (c) JJA (lower left), and (d) SON (lower right).

5.5 Summary and Conclusion

The relationship between four teleconnections (NAO, ENSO, QBO, and AMM) and the spatial and temporal variation of TCP in NAT and its sub-basins over the period from 1998 to 2011 was investigated. Linear regression models were constructed to identify the relationship between these climate factors and TCP.

There is generally a weak relationship between TCP and almost all of the teleconnections. AMM has the strongest correlation with TCP, especially in the Caribbean. The positive AMM is related to increases in TCP. The correlation between NAO and temporal is weaker than AMM, but it still has some interesting patterns. In May to June, the results show correlations between NAO and TCP with opposing signs in different sub-basins. In the Caribbean there is a negative correlation between TCP and May-June NAO, while there is a positive correlation along the U.S. east coast.

In contrast to previous work, ENSO is not the most important teleconnection in this region. The correlation between ENSO and seasonal TCP is not particularly strong. However, the sign of the relationship does agree with previously published literature.

There is not a statistically significant correlation between TCP and QBO during 1998 to 2011. The result is confirms previous research (e.g., Camargo and Sobel 2010) that demonstrated that the relationship between TC activity and QBO weakened after 1980s.

In terms of spatial variations of TCP, May-June NAO was found to influence the TC precipitation in the East Coast and Caribbean by influencing the occurrence of

straight moving hurricanes. When May to June NAO is positive, there tends to be more TCP in the East Coast and less in the Caribbean region.

There is greater TC precipitation within La Niña years in the majority NAT. However, TCP is greater in El Niño years in the eastern GMX, southeastern of United States, and North Caribbean Sea. Those results are in accord with previous researches(Jiang and Zipser 2009; Rodgers et al. 2001).

QBO shows similar pattern with NAO, it has an opposite impact on ECO and GMX or CAR. TCP is greater in positive QBO years in the ECO. However, during negative QBO years, TC rainfall is greater over CAR, southern part of continent of North America, Gulf of Mexico. The physical explanation of impact of QBO is still uncertain.

TCP in positive AMM years is much greater than in negative AMM years. AMM is positively associated with SST, LLV and convergence, while it is negatively associated with SLP and VWS. Therefore, AMM is an indicator of Atlantic climatic conditions that are closely connected with TCP.

In the analysis of spatial correlation, the relationship between ENSO and TCP is highly seasonal variable. In DJF, the significant correlations between AMM and TCP are rare in NAT. However, there are statistically significant correlations in MAM, JJA and SON. Almost all of these correlations are positive in the NAT basin. For QBO and NAO, there are fewer statistically significant correlations in the study region.

CHAPTER VI

CONCLUSIONS AND FUTURE RESEARCH

6.1 Conclusion

TCP is associated with extreme precipitation events and damaging floods. People living in coastal areas in the Atlantic are frequently effected by TCP. This study developed a TCP climatology and documented the temporal and spatial patterns of TCP in the NAT and its sub-basins. This study also investigated the relationships between four climatic oscillations (NAO, ENSO, QBO, and AMM) and TCP.

The spatial patterns of TCP are consistent with past studies (Rodgers et al. 2001, Jiang and Zipser 2010,). TCs contribute an average of 76 mm precipitation per year in the North Atlantic. Among the sub-basins, TCP occurs greatest in the GMX (140 mm per year). Ocean and coastal areas typically received more TCP than inland areas. Generally, TCP corresponds with the storm tracks. In this study, no statistically significant trends in TCP volume, total rainfall, and TCP fraction were found in the NAT between 1998 and 2011. This differs from previous research. However, there is strong correlation between TCP and TC frequency and intensity.

Generally, there are weak correlations between almost all of the teleconnections and TCP. AMM has the strongest correlation with TCP, especially in the CAR region. There is positive correlation between TCP and AMM over the period of the hurricane season. The relationship between NAO and May to June TCP varies by sub-basin because the NAO influences hurricane tracks. There tends to be more TCP in the CAR and less in the ECO when the May-June NAO is strongly positive. ENSO is not the most

important teleconnection in the NAT. However, TCP tends to increase within the La Niña phase. The correlation between QBO and the TCP is essentially zero. This finding agrees with the previous research (Camargo and Sobel 2010) that suggests there is no correlation between QBO and TC activity after 1980s.

6.2 Implications

Satellite-estimated TCP (1998 to 2011) was used to develop a TCP climatology for the NAT. Satellite-derived precipitation data is useful for identifying the spatial patterns in TCP patterns. It is important to quantify the variability of the TCP because it helps to improve our understanding of how and why TCP varies on interannual to decadal timescales. This information is significant for planning and policy making in coastal communities. This study found that the spatial patterns and temporal variability of TCP are consistent with previous studies even though the data sources and time periods of analysis are different.

Teleconnections are responsible for a significant amount of the interannual variation in TCP in the NAT and in all of the sub-basins. This study helps to identify the teleconnections that should be included in statistical models of TCP in the NAT. These statistical models may be able to forecast variations in TCP. The impact of the climatic factors on TCP was also clarified in the study. For example, it appears that the previously reported relationships between TC activity and QBO may be spurious. An better understanding of the physical mechanisms that in charge of TCP will help us to predict how climate change may impact TCP.

6.3 Limitations

There are several limitations in this study. First, our TCP dataset only includes 14 seasons (1998-2011) of data. The small sample size has an impact on the robustness of the statistical analysis. For example, it is unclear whether the lack of a relationship between TCP and the QBO result from the short-period of record, or the lack of a physical connection. Second, there are some limitations with the TCPF dataset. There is tendency for 3B42 to over-estimate the rain rate due to the relatively low spatial resolution (Jiang and Zipser 2010). Also, some storms were missed by TRMM version 7. Third, a number of the teleconnections may not be independent of each other. In this study, the influence of each teleconnection is considered independently. We have not considered the joint influences (constructive or desctructive) of the teleconnections.

6.4 Future Research

Continued study of TCP is still needed. Future research should focus on developing a monthly TCP climatology. It is also necessary to identify both of the spatial and temporal patterns of TCP over longer timescales to determine whether there are significant trends or geographic shifts in TCP patterns. Therefore, using a merged gauge and satellite precipitation products may be helpful for putting recent activity into a long-term perspective. In addition, the relationships between climate oscillations and TCP could be used to develop multivariate statistical models to forecast seasonal TCP (i.e., similar to Zhu et al. 2013b). Finally, an improved quantification of TCP and TCP risk can enhance understanding of flooding risk and these data can be used as input in hydrologic models to identify the impacts of TCP on flooding at the local scale.

REFERENCES

Adler, R. F., G. J. Huffman, A. Chang, R. Ferraro, P. Xie, J. Janowiak, B. Rudolf, U. Schneider, S. Curtis, D. Bolvin, A. Gruber, J. Susskind, and P. Arkin (2003), The Version 2 Global Precipitation Climatology Project (GPCP) Monthly Precipitation Analysis (1979-Present). *Journal of Hydrometeorology,* 4,1147-1167, doi: http://dx.doi.org/10.1175/1525-7541(2003)004<1147:TVGPCP>2.0.CO;2

Adler, R. F., G. J. Huffman, D. T. Bolvin, S. Curtis, and E. J. Nelkin (2000), Tropical Rainfall Distributions Determined Using TRMM Combined with Other Satellite and Rain Gauge Information. *Journal of Applied Meteorology,* 39, 2007-2023, doi: http://dx.doi.org/10.1175/1520-0450(2001)040<2007:TRDDUT>2.0.CO;2

Adler, R. F., H. M. Yeh, N. Prasad, W. Tao, and J. Simpson (1991), Microwave Simulations of a Tropical Rainfall System with a Three-Dimensional Cloud Model. *Journal of Applied Meteorology,* 30**,** 924-953, doi: http://dx.doi.org/10.1175/1520-0450-30.7.924

Barlow, M. (2011), Influence of Hurricane-Related Activity on North American Extreme Precipitation. *Geophysical Research Letters,* 38**,** L04705, doi: 10.1029/2010GL046258

Bell, G. D., M. S. Halpert, R. C. Schnell, R. W. Higgins, J. Lawrimore, V. E. Kousky, R. Tinker, W. Thiaw, M. Chelliah, and A. Artusa (2000), Climate Assessment for 1999. *Bulletin of the American Meteorological Society*, 81, s1–s50, doi: http://dx.doi.org/10.1175/1520-0477(2000)81[s1:CAF]2.0.CO;2

Beven II, J. L., L. A. Avila, E. S. Blake, D. P. Brown, J. L. Franklin, R, D. Knabb, Richard J. Pasch, Jamie R. Rhome, and Stacy R. Stewart, (2008), Atlantic Hurricane Season of 2005. *Monthly Weather Review*, 136, 1109–1173, doi: http://dx.doi.org/10.1175/2007MWR2074.1

Camargo, S. J., and A. H. Sobel (2010), Revisiting the Influence of the Quasi-Biennial Oscillation on Tropical Cyclone Activity. *Journal of Climate*, 23(21), 5810-5825, doi:10.1175/2010jcli3575.1.

Cerveny, R. S., and L. E. Newman (2000), Climatological Relationships between Tropical Cyclones and Rainfall. *Monthly Weather Review,* 128**,** 3329-3336, doi: http://dx.doi.org/10.1175/1520-0493(2000)128<3329:CRBTCA>2.0.CO;2

Chang, C.P., Y. T. Yang, and H. C. Kuo (2013), Large Increasing Trend of Tropical Cyclone Rainfall in Taiwan and the Roles of Terrain. *Journal of Climate*, 26, 4138–4147, doi: http://dx.doi.org/10.1175/JCLI-D-12-00463.1

Chen, J. M., T. Li, and C. F. Shih (2010), Tropical Cyclone and Monsoon-Induced Rainfall Variability in Taiwan. *Journal of Climate,* 23**,** 4107-4120, doi: http://dx.doi.org/10.1175/2010JCLI3355.1

Cheung, K. K. W., L. R. Huang, and C. S. Lee(2008), Characteristics of Rainfall during Tropical Cyclone Periods in Taiwan. *Natural Hazards and Earch System Sciences*, 8, 1463-1474, doi:10.5194/nhess-8-1463-2008

Chiang, J. C. H., and D. J. Vimont (2004), Analogous Pacific and Atlantic Meridional Modes of Tropical Atmosphere-Ocean Variability. *Journal of Climate,* 17, 4143 – 4158, doi: http://dx.doi.org/10.1175/JCLI4953.1

Dare, R. A., N. E. Davidson, and J. L. McBride (2012), Tropical Cyclone Contribution to Rainfall over Australia. *Monthly Weather Review,* 140**,** 3606-3619, doi: http://dx.doi.org/10.1175/MWR-D-11-00340.1

Elsner, J.B. (2003), Tracking Hurricanes. *Bulletin of the American Meteorolgical Society, 84, 353–356*, doi: http://dx.doi.org/10.1175/BAMS-84-3-353

Elsner, J.B., and T.H.Jagger (2006), Prediction Models for Annual U.S. Hurricane Counts. *Journal of Climate*, 19: 2935- 2952, doi: http://dx.doi.org/10.1175/JCLI3729.1

Emanuel, K. A. (2013), Downscaling CMIP5 Climate Models Shows Increased Tropical Cyclone Activity over the 21st century. *Proceedings of the National Academy of Sciences U.S.A.*, 110(30), 12,219–12,224, doi:10.1073/pnas.1301293110.

Englehart, P. J., and A. V. Douglas (2001), The Role of Eastern North Pacific Tropical Storms in the Rainfall Climatology of Western Mexico. *International Journal of Climatology,* 21, 1357-1370, doi: 10.1002/joc.637

Goldenberg, S. B., and L. J. Shapiro (1996), Physical Mechanisms for the Association of El Niño and West African Rainfall with Atlantic Major Hurricane Activity. *Journal of Climate*, 9, 1169–1187. doi: http://dx.doi.org/10.1175/1520-0442(1996)009<1169:PMFTAO>2.0.CO;2

Gray, W. M. (1984a), Atlantic Seasonal Hurricane Frequency .1. El-Nino and 30-Mb Quasi-Biennial Oscillation Influences. *Monthly Weather Review*, 112(9), 1649-1668, doi:10.1175/1520-0493(1984)112<1649:ASHFPI>2.0.CO;2.

Gray, W. M. (1984b), Atlantic Seasonal Hurricane Frequency. 2. Forecasting Its Variability. *Monthly Weather Review*, 112(9), 1669-1683, doi:10.1175/1520-0493(1984)112<1669:ASHFPI>2.0.CO;2.

Grimes, D. I. F., E. Pardo-Iguzquiza, and R. Bonigacio (1999), Optimal Areal Rainfall Estimation Using Raingauges and Satellite Data. *Journal of Hydrology,* 222, 93 - 108, doi: http://dx.doi.org/10.1016/S0022-1694(99)00092-X

Gualdi, S., E. Scoccimarro, and A. Navarra (2008), Changes in Tropical Cyclone Activity due to Global Warming: Results from a High-resolution Coupled General Circulation Model. *Journal of Climate*, 21, 5204–5228, doi: http://dx.doi.org/10.1175/2008JCLI1921.1

Henderson-Sellers, A., H. Zhang, G. Berz, K. Emanuel, W. Gray, C. Landsea, G. Holland, J. Lighthill, S. L. Shieh, P. Webster, and K. McGuffie (1998), Tropical Cyclones and Global Climate Change: A Post-IPCC Assessment. *Bulletin of the American Meteorological Society,* 79**,** 19-38, doi: http://dx.doi.org/10.1175/1520-0477(1998)079<0019:TCAGCC>2.0.CO;2

Huffman, G. J., D. T. Bolvin, E. J. Nelkin, D. B. Wolff, R. F. Adler, G. Gu, Y. Hong, K. P. Bowman, and E. F. Stocker (2007), The TRMM Multisatellite Precipitation Analysis (TMPA): Quasi-global, multiyear, combined-sensor precipitation estimates at fine scales. *Journal of Hydrometeorology*, 8, 38–55, doi: http://dx.doi.org/10.1175/JHM560.1

Jarvinen, B. R., C. J. Neumann, and M. A. S. Davis (1984), A Tropical Cyclone Data Tape for the North Atlantic Basin, 1886 – 1983: *Contents, limitations and uses*. Technical Memorandum NWS NHC-22, 21 pp., NOAA, Silver Spring, Md

Jiang, H., C. Liu, and E. J. Zipser (2011), A TRMM-based Tropical Cyclone Cloud and Precipitation Feature Database. *Journal of Climate and Applied Meteorology*, 50,1255-1274, doi: 10.1175/2011JAMC2662.1

Jiang, H., and E. J. Zipser (2010), Contribution of Tropical Cyclones to the Global Precipitation from Eight Seasons of TRMM Data: Regional, Seasonal, and Interannual Variations. *Journal of Climate,* 23**,** 1526-1543, doi: http://dx.doi.org/10.1175/2009JCLI3303.1

Jones, P. D., T. Jónsson and D. Wheeler (1997), Extension to the North Atlantic Oscillation Using Early Instrumental Pressure Observations from Gibraltar and South-West Iceland. *International Journal of Climatology*, 17: 1433-1450, DOI: 10.1002/(SICI)1097-0088(19971115)17:13<1433::AID-JOC203>3.0.CO;2-P

Kim, J. H., C. H. Ho, M. H. Lee, J. H. Jeong, and D. Chen (2006), Large Increase in Heavy Rainfall Associated with Tropical Cyclone Landfalls in Korea after the Late 1970s. *Geophysical Research Letters*, 33, L18706, doi:10.1029/2006GL027430.

Klotzbach, P. J., and W. M. Gray (2003), Forecasting September Atlantic Basin Tropical Cyclone Activity. *Weather Forecast*, *18*(6), 1109-1128, doi: 10.1175/1520-0434(2003)018<1109:FSABTC>2.0.CO;2.

Knaff, J. A., (1997), Implications of Summertime Sea Level Pressure Anomalies in the Tropical Atlantic Region. *Journal of Climate*, 10, 789–804, doi: http://dx.doi.org/10.1175/1520-0442(1997)010<0789:IOSSLP>2.0.CO;2

Knight, D. B. and R. E. Davis (2009), Contribution of Tropical Cyclones to Extreme Rainfall Events in the Southeastern United States. *Journal of Geophysical Research*, 114, D23102, doi:10.1029/2009JD012511

Knutson, T. R., J. L. McBride, J. Chan, K. Emanuel, G. Holland, C. Landsea, I. Held, J. P. Kossin, A. K. Srivastava, and M. Sugi (2010), Tropical Cyclones and Climate Change. *Nature Geoscience*, 3, 157-163, doi:10.1038/ngeo779

Knutson, T. R., J. J. Sirutis, S. T. Garner, G. A. Vecchi, and I. M. Held(2008), Simulated Reduction in Atlantic Hurricane Frequency under Twenty-first-century Warming conditions. *Nature Geoscience*, 1, 359–364, doi:10.1038/ngeo202

Kossin, J. P., S. J. Camargo, and M. Sitkowski (2010), Climate Modulation of North Atlantic Hurricane Tracks. *Journal of Climate,* 23(11), 3,057–3,076, doi: http://dx.doi.org/10.1175/2010JCLI3497.1

Kubota, H. and B. Wang (2009), How Much Do Tropical Cyclones Affect Seasonal and Interannual Rainfall Variability over the Western North Pacific? *Journal of Climate,* 22, 5495-5510, doi: http://dx.doi.org/10.1175/2009JCLI2646.1

Kuleshov, Y., L. Qi, R. Fawcett, and D. Jones (2008), On Tropical Cyclone Activity in the Southern Hemisphere: Trends and the ENSO connection. *Geophysical Research Letters*, 35, L14S08, doi:10.1029/ 2007GL032983.

Kummerow, C., J. Simpson, O. Thiele, W. Barnes, A. T. C. Chang, E. Stocker, R. F. Adler, A. Hou, R. Kakar, F. Wentz, P. Ashcroft, T. Kozu, Y. Hong, K. Okamoto, T. Iguchi, H. Kuroiwa, E. Im, Z. Haddad, G. Huffman, B. Ferrier, W. S. Olson, E. Zipser, E. A. Smith, T. T. Wilheit, G. North, T. Krishnamurti, and K. Nakamura, (2000), The Status of the Tropical Rainfall Measuring Mission (TRMM) after Two Years in Orbit. *Journal of Applied Meteorology*, 39, 1965–1982, doi: http://dx.doi.org/10.1175/1520-0450(2001)040<1965:TSOTTR>2.0.CO;2

Kunkel, K. E., D. R. Easterling, D. A. R. Kristovich, B. Gleason, L. Stoecker, and R. Smith (2010), Recent Increases in U.S. Heavy Precipitation Associated with Tropical Cyclones. *Geophysical Research Letters*, 37, L24706, doi: 10.1029/2010GL045164

Lau, K. M., and Y. P. Zhou (2012), Observed Recent Trends in Tropical Cyclone Rainfall over the North Atlantic and the North Pacific. *Journal of Geophysical Research*, 117, D03104, doi:10.1029/2011JD016510

Lau, K. M., Y. P. Zhou, and H. T. Wu (2008), Have Tropical Cyclones been Feeding more Extreme Rainfall? *Journal of Geophysical Research: Atmospheres,* 113**,** D23113, doi: 10.1029/2008JD009963

Landsea, C. W., D. A. Glenn, W. Bredemeyer, M. Chenoweth, R. Ellis, J. Gamache, L. Hufstetler, C. Mock, R. Perez, R. Prieto, J. Sánchez-Sesma, D. Thomas, and L. Woolcock (2008), A Reanalysis of the 1911–20 Atlantic Hurricane Database. *Journal of Climate*, 21, 2138–2168, doi: http://dx.doi.org/10.1175/2007JCLI1119.1

Landsea, C. W., R. A. Pielke Jr., A. M. Mestas-Nuñez, and J. A. Knaff (1999), Atlantic Basin Hurricanes: Indices of Climatic Changes. *Climatic Change*, 42, 89–129, doi: 10.1023/A:1005416332322

Lonfat, M., F. D. Marks, and S. S. Chen (2004), Precipitation Distribution in Tropical Cyclones Using the Tropical Rainfall Measuring Mission (TRMM) Microwave Imager: A Global Perspective. *Monthly Weather Review,* 132**,** 1645-1660. doi: http://dx.doi.org/10.1175/1520-0493(2004)132<1645:PDITCU>2.0.CO;2

NOAA (National Oceanic and Atmospheric Administration) (2014), The Atlantic Hurricane Database Re-analysis Project. www.aoml.noaa.gov/hrd/hurdat/comparison_table.html.

Nogueira, R. C., and B. D. Keim (2010), Annual Volume and Area Variations in Tropical Cyclone Rainfall over the Eastern United States. *Journal of Climate*, 23, 4363-4374, doi: http://dx.doi.org/10.1175/2010JCLI3443.1

Pasch,R. J., M. B. Lawrence, L. A. Avila, J. L. Beven, J. L. Franklin, and S. R. Stewart (2004), Atlantic Hurricane Season of 2002. *Monthly Weather Review*, 132, 1829–1859.doi: http://dx.doi.org/10.1175/1520-0493(2004)132<1829:AHSO>2.0.CO;2

Patricola, C. M., R. Saravanan, and P. Chang (2014), The Impact of the El Niño–Southern Oscillation and Atlantic Meridional Mode on Seasonal Atlantic Tropical Cyclone Activity. *Journal of Climate*, 27, 5311–5328, doi: http://dx.doi.org/10.1175/JCLI-D-13-00687.1

Prat, Olivier P., and B. R. Nelson (2013), Precipitation Contribution of Tropical Cyclones in the Southeastern United States from 1998 to 2009 Using TRMM Satellite Data. *Journal of Climate*, 26, 1047–1062, doi: http://dx.doi.org/10.1175/JCLI-D-11-00736.1

Rappaport, E. N. (2000), Loss of Life in the United States Associated with Recent Atlantic Tropical Cyclones. *Bulletin of the American Meteorological Society,* 81**,** 2065-2073, doi: http://dx.doi.org/10.1175/1520-0477(2000)081<2065:LOLITU>2.3.CO;2

Ren, F., G. Wu, W. Dong, X. Wang, Y. Wang, W. Ai, and W. Li (2006), Changes in Tropical Cyclone Precipitation over China. *Geophysical Research Letters,* 33**,** L20702, DOI: 10.1029/2006GL027951

Rodgers, E. B., R. F. Adler, and H. F. Pierce (2000), Contribution of Tropical Cyclones to the North Pacific Climatological Rainfall as Observed from Satellites. *Journal of Applied Meteorology,* 39, 1658-1678, doi: http://dx.doi.org/10.1175/1520-0450(2000)039<1658:COTCTT>2.0.CO;2

Rodgers, E. B., R. F. Adler,and H. F. Pierce (2001), Contribution of tropical cyclones to the North Atlantic climatological rainfall as observed from satellites. *Journal of Applied Meteorology*, 40, 1785–1800, doi: http://dx.doi.org/10.1175/1520-0450(2001)040<1785:COTCTT>2.0.CO;2

Rodgers, E. B., S. W. Chang, and H. F. Pierce (1994), A Satellite Observational and Numerical Study of Precipitation Characteristics in Western North Atlantic Tropical Cyclones. *Journal of Applied Meteorology*, 33, 129-139, doi: http://dx.doi.org/10.1175/1520-0450(1994)033<0129:ASOANS>2.0.CO;2

Sabbatelli, T. A. and Mann, M. E. (2007), The Influence of Climate State Variables on Atlantic Tropical Cyclone Occurrence rates. *Journal of Geophysical Research-atmospheres*, 112(D17), doi:10.1029/2007JD008385.

Schumacher, C., and R. A. Houze (2003), Stratiform rain in the Tropics as seen by the TRMM precipitation radar. *Journal of Climate*, 16, 1739-1756, doi: http://dx.doi.org/10.1175/1520-0442(2003)016<1739:SRITTA>2.0.CO;2

Shapiro, L. J., (1989), The Relationship of the Quasi-Biennial Oscillation to Atlantic Tropical Storm Activity. *Monthly Weather Review*,117, 1545-1552, doi: http://dx.doi.org/10.1175/1520-0493(1989)117<1545:TROTQB>2.0.CO;2

Shapiro, L. J., and S. B. Goldenberg (1998), Atlantic Sea Surface Temperatures and Tropical Cyclone Formation. *Journal of Climate*, 11, 578-590, doi: http://dx.doi.org/10.1175/1520-0442(1998)011<0578:ASSTAT>2.0.CO;2

Shepherd, J. M., A. Grundstein, and T. L. Mote (2007), Quantifying the Contribution of Tropical Cyclones to Extreme Rainfall along the Coastal Southeastern United States. *Geophysical Research Letters*, 34, L23810, doi:10.1029/2007GL031694.

Simpson, J., R. F. Adler, and G. R. North (1988), A Proposed Tropical Rainfall Measuring Mission (TRMM) Satellite. *Bulletin of the American Meteorological Society,* 69, 278-295, doi: http://dx.doi.org/10.1175/1520-0477(1988)069<0278:APTRMM>2.0.CO;2

Smith, S. R., J. Brolley, J. J. O'Brien, and C. A. Tartaglione (2007), ENSO's Impact on Regional U.S. Hurricane Activity. *Journal of Climate*, 20, 1404–1414, doi: http://dx.doi.org/10.1175/JCLI4063.1

Swiss, R. E. (2010), Natural Catastrophes and Man-Made Disasters in 2009, Catastrophes Claim Fewer Victims, Insured Losses Fall,. *Sigma Study*, No 1/2010.

Trenberth, K.E. (1997),The Definition of El Niño. *Bulletin of the American Meteorological society*, 78, 2771–2777, doi: http://dx.doi.org/10.1175/1520-0477(1997)078<2771:TDOENO>2.0.CO;2

Vimont, D. J., and J. P. Kossin (2007),The Atlantic Meridional Mode and Hurricane Activity. *Geophysical Research Letters*, 34, L07709, doi:10.1029/2007GL029683.

Wolter, K. (1987), The Southern Oscillation in Surface Circulation and Climate over the tropical Atlantic, Eastern Pacific, and Indian Oceans as Captured by Cluster Analysis. *Journal of Applied Meteorology*, 26, 540–558, doi: http://dx.doi.org/10.1175/1520-0450(1987)026<0540:TSOISC>2.0.CO;2

Wolter, K., and M. S. Timlin (1993), Monitoring ENSO in COADS with a Seasonally Adjusted Principal Component Index. Proc. of the 17th Climate Diagnostics Workshop, Norman, OK, NOAA/NMC/CAC, NSSL, Oklahoma Clim. Survey, CIMMS and the School of Meteor., Univ. of Oklahoma, 52-57.

Wolter, K., and M. S. Timlin, (1998), Measuring the Strength of ENSO Events - How Does 1997/98 Rank? *Weather,* 53, 315-324, doi: 10.1002/j.1477-8696.1998.tb06408.x

Wu, Y., S. Wu, and P. Zhai (2007), The Impact of Tropical Cyclones on Hainan Island's Extreme and Total Precipitation. *International Journal of Climatology*, 27,1059 – 1064, doi: 10.1002/joc.1464

Xie, P., J. E. Janowiak, P. A. Arkin, R. Adler, A. Gruber, R. Ferraro, G. J. Huffman, and S. Curtis (2003), GPCP Pentad Precipitation Analyses: An Experimental Dataset Based on Gauge Observations and Satellite Estimates. *Journal of Climate,* 16**,** 2197-2214, doi: http://dx.doi.org/10.1175/2769.1

Xie, L., T. Yan, L. J. Pietrafesa, J. M. Morrison, and T. Karl (2005), Cliamtology and Interannual Variability of North Atlantic Hurricane Tracks. *Journal of Climate*, 18, 5370 – 5381, doi: http://dx.doi.org/10.1175/JCLI3560.1

Yokoyama, C., and Y. N. Takayabu (2008), A Statistical Study on Rain Characteristics of Tropical Cyclones Using TRMM Satellite Data. *Monthly Weather Review,* 136, 3848-3862, doi: http://dx.doi.org/10.1175/2008MWR2408.1

Zhu, L., O. Frauenfeld., and S. Quiring (2013), Seasonal Tropical Cyclone Precipitation (TCP) in Texas: A Statistical Modeling Approach based on a 60-year Climatology. *Journal of Geophysical Research–Atmospheres.* 118,8842-8856, doi: 10.1002/jgrd.50663

Zhu, L., and S. Quiring (2013), Variations in Tropical Cyclone Precipitation in Texas (1950 to 2009). *Journal of Geophysical Research Atmospheres*. 118, 3085-3096, doi:10. 1029/2012JD018554